Nile Decision Support Tool
Agricultural Planning

Burundi
Congo
Egypt
Eritrea
Ethiopia
Kenya
Rwanda
Sudan
Tanzania
Uganda

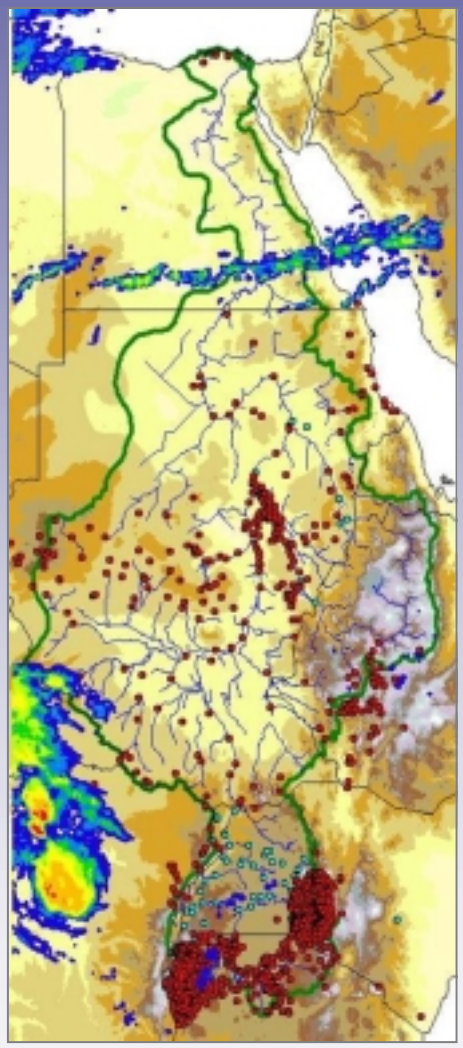

Developed collaboratively by

The Nile Basin Nations,

The Georgia Water Resources Institute at the Georgia Institute of Technology,

and

The Food and Agriculture Organization of the United Nations

June 2003

Nile Decision Support Tool (Nile DST)
Agricultural Planning

Report developed by

Kelly Brumbelow
Research Engineer

Stephen Bourne
Research Associate

Aris Georgakakos
Project Director

Georgia Water Resources Institute
School of Civil and Environmental Engineering
Georgia Institute of Technology

In collaboration with

The Nile Basin Nations

and

The Food and Agriculture Organization (FAO)
of the United Nations
Nile Basin Water Resources Project (GCP/INT/752/ITA)

June 2003

Acknowledgements

This report and associated software were developed by the Georgia Water Resources Institute (GWRI) at the Georgia Institute of Technology as part of the Nile Basin Water Resources Project (GCP/INT/752/ITA). This project was funded by the Government of Italy and was executed for the Nile Basin nations by the Food and Agriculture Organization (FAO) of the United Nations.

The GWRI Director and project staff are grateful to the Nile Basin nations (Burundi, Congo, Egypt, Eritrea, Ethiopia, Kenya, Rwanda, Sudan, Tanzania, and Uganda), their focal point institutions, their Project Steering Committee (PSC) members, and their National Modelers for entrusting us to work with them in this important basin-wide project. The development of databases, models, technical reports, software, and user manuals are key but not the only project accomplishments. Even more important are the evolving contributions relating to people and the difference the project is poised to make in data and information sharing, developing a common knowledge base for policy debates, and long term capacity building.

GWRI is also grateful to the Government of Italy and to FAO for sponsoring this project and for providing dependable logistical and technical support through the FAO offices in Rome and Entebbe.

It is our hope that the Nile DST effort will contribute in some positive way to the historic process of the Nile Basin nations to create a sustainable and peaceful future.

Aris Georgakakos
GWRI Director
Atlanta, June 2003

Disclaimer and Copyright Notice

Table of Contents

Agricultural Planning Module

1. Introduction

The Nile DST Agricultural Planning Module is a comprehensive software useful for purposes of planning and assessment of crop yields and irrigation needs for a variety of crops. The module combines advanced models of plant physiology and irrigation optimization algorithms with database and geographic information systems in a user-friendly manner. Questions involving the agricultural productivity of irrigation water can be evaluated for a wide range of climatic conditions for locations throughout the Nile Basin. Furthermore, plans for irrigation needs for crop rotations and irrigation district management can be evaluated using the system.

The Agricultural Planning module is intended to function in a complementary fashion with the other modules of the Nile DST. Water availability for irrigation can be modeled in the Hydrology module. Climatic patterns can be determined in the Data Analysis module and then used to help shape agricultural assessments. Scenarios of water releases and withdrawals developed in the River Basin Management module can be assessed for their agricultural consequences.

This technical report describes the background, development, and scientific principles contained in the Nile DST Agricultural Planning module. Knowledge of these aspects will help the user to understand how the module works and the best ways to use it. Specific directions on software use are further described in the Nile DST User's Manual.

2. Irrigation planning

The Nile DST Agricultural Planning module principally uses the relationship of crop yield to irrigation for various assessments. This relationship is known as the "crop-water production function" (CWPF). Derivation of CWPF's can be accomplished in multiple ways in the software, and the methods available are fully described in Section 4. As use of CWPF's is a relatively recent development, it is useful to discuss traditional methods of irrigation planning as well. These techniques, usually collected as reference evapotranspiration-crop coefficient methods, are also available in the Nile DST as an option to use the FAO CROPWAT methods. Section 2.1 focuses on the traditional techniques.

2.1. Traditional Methods

The concept of analysis of crop production using a water production function is relatively new and is a product of increasingly limited water resources. In the past, irrigation planning has proceeded on the implicit assumption that the water demands of

crops should be "fully" met, and no substantial regard was given to how much could be grown with lesser irrigation depths. The Blaney-Criddle (1950) method was one of the earliest procedures for calculating crop water "requirements." The original form of the method determined monthly water requirements as empirical crop coefficients multiplied by the summation over the growing season of the monthly products of mean monthly temperature and monthly percentage of total annual daylight hours. Thus, necessary applied water was a function of climatic norms at the monthly scale and past experience with various crops. Subsequent revisions of Blaney-Criddle allowed estimation of water needs on shorter time-scales, i.e., 5 to 30 days (USDA 1970), and the inclusion of wind speed and minimum daily relative humidity (Doorenbos and Pruitt 1977, Allen and Pruitt 1986). Even with its revisions, the Blaney-Criddle method relies on heavily aggregated data and empiricisms, disregards many important factors (e.g., temporal distribution of applied water, soil conditions, weather anomalies, etc.), and can give no information needed for the development of a crop-water production function.

Since the majority of water used by crops is evapotranspired – water used for building biomass is very small by comparison – several methods to compute crop water needs based on hydrologic conceptions of evapotranspiration (ET) have evolved. Hydrologic formulations of evapotranspiration have developed over the past fifty years with several milestones. Penman (1948) combined radiative (energy) and mass transfer (aerodynamic) effects to compute potential evaporation (PE), i.e., evaporation from a free water surface with no shortage of water. Monteith (1965) extended this "combination" approach to include aerodynamic roughness (boundary layer effects) and stomatal resistance to transpiration to determine potential evapotranspiration (PET) from a reference crop, usually well-watered grass or alfalfa. Priestly and Taylor (1972) concluded from experimental evidence that only the radiative transfer term from Penman's equation (multiplied by a constant) was necessary to calculate ET from large, uniformly wet surfaces. Other important estimations of PET have been proposed by Thornthwaite (1948), Turc (1961), and Jensen (1966), among others. In addition to theoretical methods, improved ability to correlate direct pan measurements of evaporation to reference crop ET has been developed over the past several decades (Linsley et al. 1982, Doorenbos and Pruitt 1977). ASCE (1990) includes a comparative study of twenty different methods of estimating PET for a wide range of locations and climatic regimes. This study concluded that the Penman-Monteith equation performed the best of all the methods when predictions were verified against lysimeter measurements.

The ability to reliably compute PET for an agreed upon reference crop (hereafter referred to as reference evapotranspiration ET_{ref}) allowed for the development of irrigation scheduling methods where crop ET demands were known relative to ET_{ref}. Using experimental data, ratios of crop ET_c to ET_{ref} have been developed for a variety of crops:

$$K_c = \frac{ET_c}{ET_{ref}} \qquad \textbf{(1)}$$

$$ET_{crop}(t) = ET_o(t) \cdot K_{crop}(t) \quad \Rightarrow \quad I_{req}(t) = ET_{crop}(t) - P_{eff}(t)$$

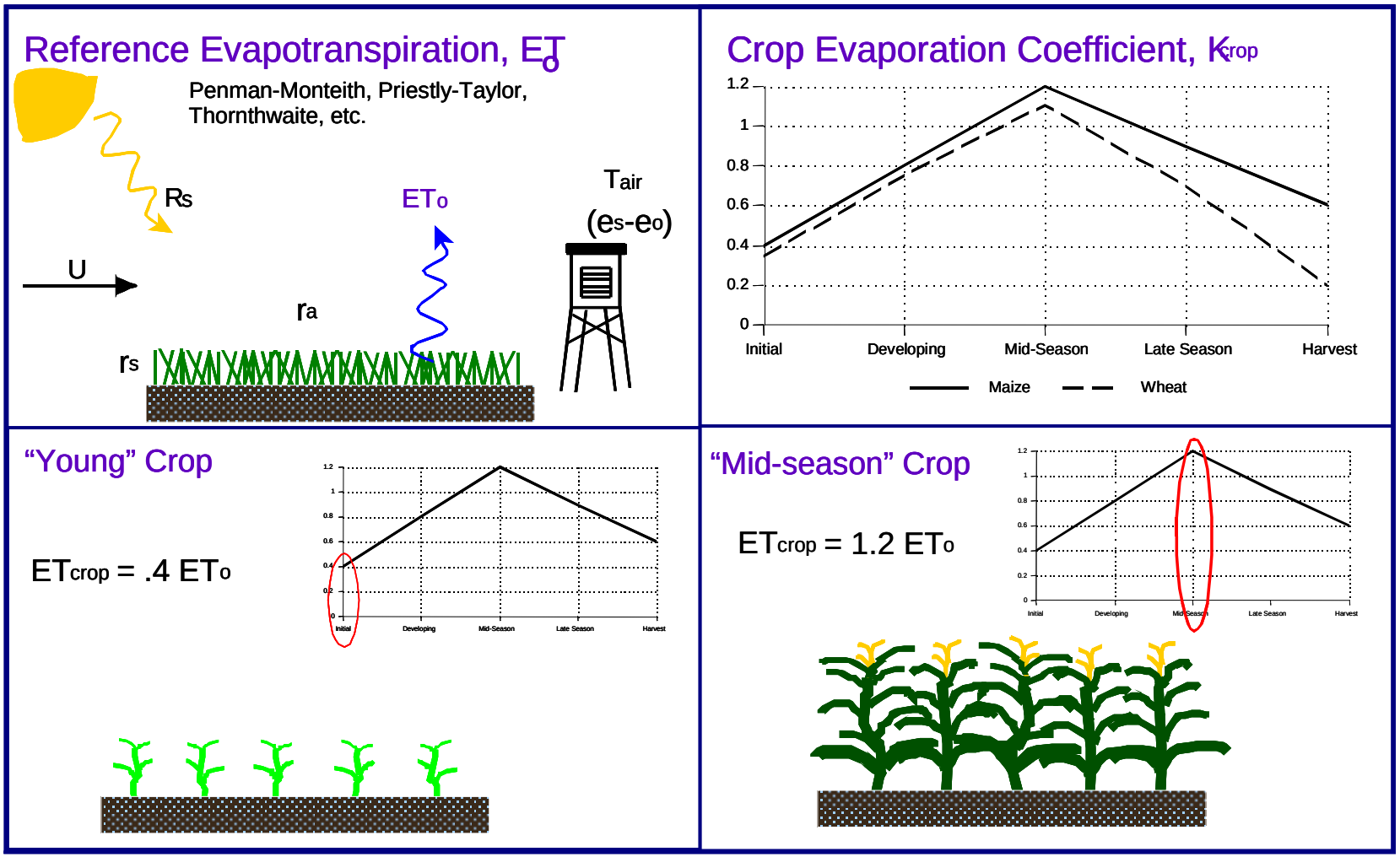

Figure 1. Reference Evapotranspiration Irrigation Scheduling

These ratios K_c, known as crop coefficients, vary with crop phenology. Typically, crop coefficients are very low at plant emergence but increase as leaf area increases towards the mid-season point. As the plant shifts growth priorities from leaf and stem growth to grain production and leaf area decreases, crop coefficients decrease. The irrigation scheduling process (see Figure 1) begins with a discretization of the growing season into specified time intervals. For each time interval climatic parameters necessary to compute ET_{ref} are obtained for the conditions desired (e.g., average conditions, specific-percentile conditions, etc.). Once values of ET_{ref} are known for each time interval, anticipated crop ET_c for each time interval is found by multiplying ET_{ref} by the crop coefficient value in effect for the growth stage reached in the interval. Crop ET_c is then subtracted from precipitation anticipated in each interval. For each interval having a positive difference between crop ET and infiltrated precipitation (crop ET greater than infiltrated precipitation), irrigation is scheduled for that period so that total applied water equals crop ET_c. This procedure is expressed mathematically:

$$
\begin{aligned}
&ET_{ref,t} = f_{ETref}\left(T_{\max,t}, T_{\min,t}, RH_t, R_{n,t}, u_t, etc.\right) && for\ t = 1,\ldots,n \\
&ET_{c,t} = K_{c,t} \cdot ET_{ref,t} && for\ t = 1,\ldots,n \qquad \textbf{(2)} \\
&\left.\begin{aligned} I_t &= 0 \\ I_t &= ET_{c,t} - P_t \end{aligned}\right\} if \begin{cases} P_t \geq ET_{c,t} \\ P_t < ET_{c,t} \end{cases} && for\ t = 1,\ldots,n
\end{aligned}
$$

where T_{max} is maximum temperature, T_{min} is minimum temperature, RH is relative humidity, R_n is net incoming radiation, u is wind speed, I is irrigation, and P is infiltrated precipitation and all quantities are indexed to time increments t. A complete exposition of this methodology is given by Allen et al. (1998) in FAO Irrigation and Drainage Paper 56.

The CROPWAT software (Smith 1992, Clarke 1998) produced by FAO utilizes the reference evapotranspiration method to determine crop water requirements. It also includes an irrigation scheduling method utilizing a simple soil moisture balance. Crop water requirements not supplied by infiltrated precipitation are assumed to be drawn from soil moisture. When soil water falls below user-defined limits, irrigation is scheduled. Soil water content should be modeled whenever possible as it is a potentially very important reservoir of water for the plant to use. It is not uncommon for the plant-extractable water capacity of a soil to be equal to several weeks' worth of rainfall at its locale. The concept of soil water "mining" as a means to reduce irrigation requirements has been discussed by Woodruff et al. (1972), Martin et al. (1991), and Mugabe and Nyakatawa (2000) among others. Removing that water from consideration may result in overestimation of irrigation requirements.

This traditional method of irrigation planning assumes that all crop water needs will be fully satisfied. Increasingly limited irrigation resources have refocused research priorities on scenarios of "deficit irrigation" where total applied water is less than total ET potential. The reduction in crop yield due to drought stress was assessed perhaps most famously by Doorenbos and Kassam (1979). They related yield reductions to the failure of the soil-plant-water system to meet evapotranspirative demand. Thus, their

concept of yield reduction relied heavily on the reference evapotranspiration-crop coefficient model. In quantitative terms, their yield-drought stress model was:

$$\left(1-\frac{Y_{act}}{Y_{\max}}\right)_{gs} = k_{y,gs}\cdot\left(1-\frac{ET_{act}}{ET_{\max}}\right)_{gs} \quad \textit{in each growth stage 1,…,n, and}$$

$$\left(1-\frac{Y_{act}}{Y_{\max}}\right) = 1-\prod_{gs=1}^{n}\left(\frac{Y_{act}}{Y_{\max}}\right)_{gs} \quad \textit{for the entire season,} \qquad \textbf{(3)}$$

where Y_{act} and Y_{max} are actual and maximum possible crop yield, respectively, k_y is a growth-stage-specific yield reduction coefficient, and ET_{act} and ET_{max} are actual and maximum possible crop evapotranspiration, respectively. Thus, reductions in crop yield are calculated as the product of weighted ratios of actual crop evapotranspiration to the crop evapotranspiration that would occur if water were abundant. The relative values of the growth-stage-specific yield reduction coefficients are indicative of the relative effect of drought stress on yield in each growth stage. Doorenbos and Kassam (1979) also specified a season-long model that omitted the partitioning of the season into growth stages:

$$\left(1-\frac{Y_{act}}{Y_{\max}}\right)_{season} = k_{y,season}\cdot\left(1-\frac{ET_{act}}{ET_{\max}}\right)_{season} \qquad \textbf{(4)}$$

The evapotranspiration ratio-yield reduction model has also been formulated as an additive model:

$$\frac{Y_{act}}{Y_{\max}} = \sum_{gs=1}^{n} k_{y,gs}\cdot\left(\frac{ET_{act}}{ET_{\max}}\right)_{gs} \qquad \textbf{(5)}$$

All three formulations have been popular in various studies (e.g., Paul et al. (2000), Wardlaw and Barnes (1999), and Sunantara and Ramirez (1997), among many others).

Some studies, motivated at times by unsatisfactory performance of the above functions, have investigated other formulations of the yield reduction versus ET ratio relationship. There have also been formulations of yield as a function of actual seasonal ET. For example, Dinar et al. (1986) assessed the performance of several alternative functions:

$$
\begin{aligned}
Y &= \alpha \cdot ET + \beta \cdot ET^2 + \gamma \\
\ln Y &= \alpha \cdot \ln ET + \beta \\
\ln Y &= \alpha + \sum_{gs} \beta_{gs} \cdot \ln ET_{gs} \\
\ln Y &= \alpha + \sum_{gs} \beta_{gs} \cdot \ln \left[1 - \left(1 - \frac{ET_{act,gs}}{ET_{\max,gs}} \right)^2 \right]
\end{aligned}
\qquad \textbf{(6)}
$$

Dinar et al. tested these functional forms using observed cotton growth. The R^2 values for the four functions ranged from 0.28 to 0.76 indicating that much variability in yield remained unexplained despite the large numbers of parameters in the last two functions.

Other studies have used or derived a linear function of ET to predict yield:

$$Y = \alpha \cdot ET + \beta \qquad \textbf{(7)}$$

Field studies using this form include English and Nakamura (1989). Martin et al. (1989) used a variation on the linear function:

$$Y = Y_d + \alpha \cdot \left(ET_{act} - ET_d \right) \qquad for\ ET_d \le ET_{act} \le ET_{\max} \qquad \textbf{(8)}$$

Holzapfel et al. (1990) and Caravallo et al. (1998) used a polynomial function to relate yield reduction to ET ratio:

$$\frac{Y_{act}}{Y_{\max}} = \alpha \cdot \left(\frac{ET_{act}}{ET_{\max}} \right)^{\delta} + \beta \cdot \left(\frac{ET_{act}}{ET_{\max}} \right)^{\varepsilon} + \gamma \qquad \textbf{(9)}$$

where α, β, γ, δ, and ε are coefficients whose values are determined by regression.

The usefulness of these models where yield reduction is due to reduced ET is obvious. Some of the effects of deficit irrigation practices can be quantified. However, the yield-ET model does possess some shortcomings. First, many of the model expressions include various coefficients that must be evaluated by regression. Thus, the modeler is still dependent on local data that is generally obtained with some cost. In that respect, these yield-ET models are really just mathematical summarizations of information at the level of Hexem and Heady's (1978) discussion of experimentally derived crop-water production functions. Second, many of these yield-ET functions only express yield reduction relative to maximum yield. However, there is no accompanying means by which to determine maximum yield in absolute terms. While this limitation is perhaps not crucially important in all cases at the scale of one field, consideration of irrigation allocation to many spatially distinct sites must include absolute magnitude of benefits. Third, the yield-ET model is incapable of considering other influences on crop growth beyond ET. Factors such as plant absorbable radiation, temperatures relative to

critical values, and daylength may have as much or more influence on crop yield as controllable changes in seasonal ET due to irrigation scheduling. Most importantly, the set of methods based on reference evapotranspiration are capable on their own of producing a single "snapshot" of irrigation and expected change in relative crop yield. That is, rather than develop a full picture of how crop yield changes with irrigation over a full growing season, the traditional method produces a single irrigation schedule, the schedule is not necessarily optimized to make best use of water, and the estimate of relative crop yield might be improved without changing the total irrigation amount for the season. Thus, the need for a means by which to overcome these issues is clear. The next section discusses the advantages to using fully developed CWPF's in irrigation planning.

2.2. Crop-Water Production Functions (CWPF's)

The key piece of data for decision support in irrigation planning is the crop-water production function (CWPF) that expresses grain (or fruit, lint, etc.) yield per cropped area as a function of irrigation on the cropped area. Hexem and Heady (1978) provide a classic discussion on the derivation, features, and roles of water production functions.

Figure 2 is a schematic of a CWPF that illustrates its important component parts. The horizontal axis is total irrigation applied in the growing season (units of mm or m^3/ha); the vertical axis is crop yield (units of kg/ha). Where the curve intersects the vertical axis is the non-irrigated or "rainfed" yield point. As total seasonal irrigation increases, crop yield increases in a concave-downward shape. This region of positive correspondence between yield and irrigation is known as the "deficit irrigation" region since the "full" crop water needs are not met. Eventually a point is reached where additional irrigation produces no additional crop yield; the plant has all the water that it needs. This "fully irrigated yield plateau" usually extends very far to the right on the coordinate axes. At very high levels of irrigation, soil saturation interferes with root growth and nutrient processes, and crop yield begins to decrease.

The CWPF is a very useful tool for agricultural planning at the scale of a full season. However, the function does not immediately reveal information about irrigation scheduling. It is important to understand that the CWPF represents a collection of optimized irrigation schedules, one schedule for each point in the function. That is, for a specific point on the CWPF curve, there is an irrigation schedule that sums to the given seasonal irrigation total that will produce the crop yield given by the function. As an example, in Figure 3 the yield-irrigation point (177 mm, 5416 kg/ha) is marked on the graph, and there exists an irrigation schedule that totals 177 mm of irrigation for the season and will result in crop yield equal to 5416 kg/ha. If the CWPF has been optimized, then this irrigation schedule is the best possible one for 177 mm of total irrigation under the given conditions. The irrigation schedule could not be re-ordered to produce a higher crop yield. Thus, the region above the CWPF is "infeasible" – there is no way to produce 8500 kg/ha with 177 mm of irrigation under the given conditions of weather, soil, crop type, etc. In contrast, the region below the CWPF is "sub-optimal"; one can produce 3000 kg/ha crop yield with 177 mm irrigation, but the irrigation

schedule to do so would not be as efficient as the one producing 5416 kg/ha. Thus, determination of the optimized CWPF also involves finding a set of optimized irrigation schedules for varying levels of total seasonal irrigation. The methods described in Section 4 below have been developed to accomplish this dual task: optimized irrigation scheduling and CWPF determination.

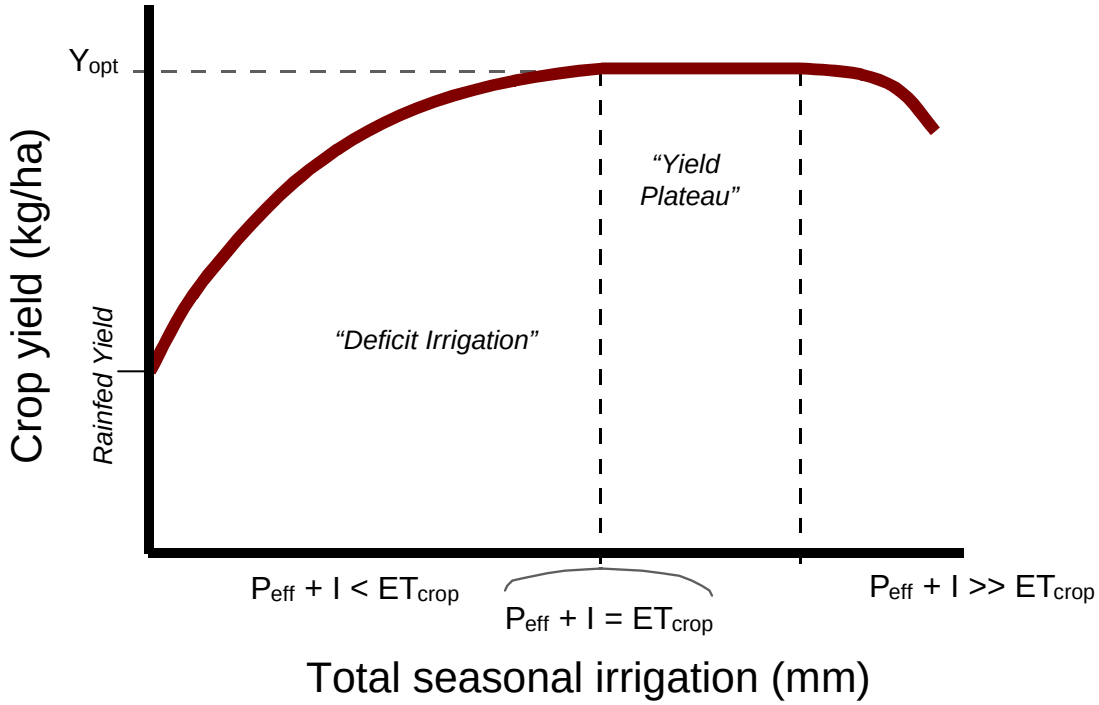

Figure 2. Schematic of a Typical Crop-Water Production Function

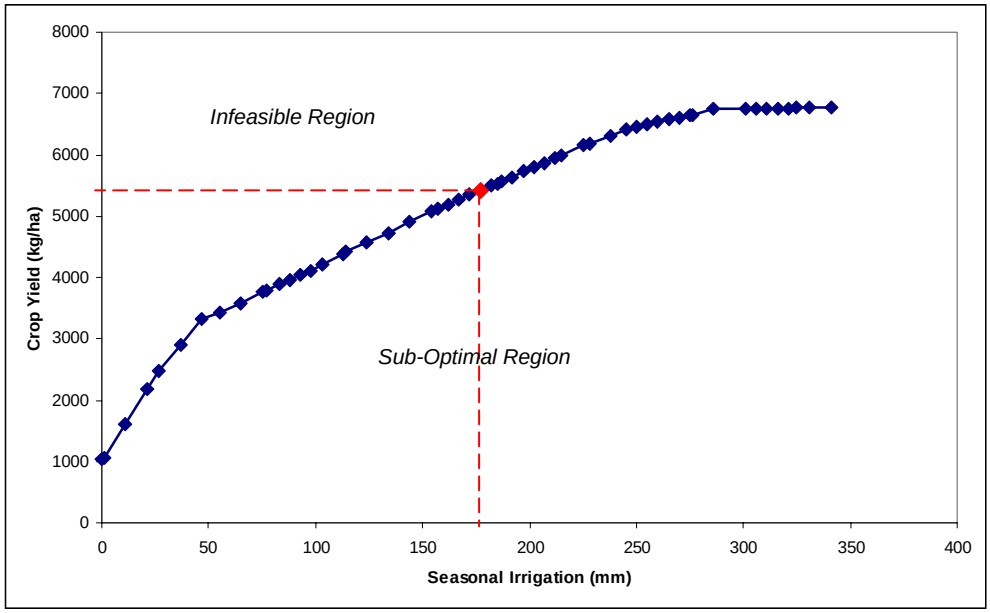

Figure 3. Example CWPF Determined by Nile DST: (177 mm, 5416 kg/ha) shown in red

Once CWPF's can be determined for a location, crops, and conditions of interest, the functions are extremely useful in agricultural planning exercises. By determining CWPF's for one crop at one site for many years of measured meteorology, a probabilistic understanding of yield and irrigation can be found. Such a probabilistic function is useful for questions of risk and reliability in agricultural operations. By comparing CWPF's for multiple crops that are to be grown either in a crop rotation or simultaneously in adjacent fields, a farmer or manager with limited irrigation resources can plan irrigation operations to maximize total yields across all crops. These types of analyses are discussed with examples in Section 5 below.

The next section discusses physiologically based crop models which are included in the Nile DST. These crop models are used for agricultural simulations and the irrigation analyses that build on these simulations.

3. Crop Models

3.1. History and Purpose of Model Development

The interest in modeling as a means to derive crop-water production functions has shared a fortunate concurrence with the emergence of robust, detailed crop growth models that numerically simulate virtually all aspects of the development of individual plants. Models such as these were not originally intended for exclusive application to irrigation planning; rather, these models were collections of various "first principles" of plant physiology that could be used to test various hypotheses. In effect, the computer models were intended to allow rapid and inexpensive experimentation that did not require large amounts of physical resources. Examples of the intended applications of these models include investigation of issues such as planting practices (planting date, seed depth, planting density, row spacing, etc.), management practices (fertilizer application scheduling, comparison of effectiveness of types of fertilizer, response to irrigation, etc.), genotype differences (yield differences among cultivars in different locations, sensitivity of specific cultivars to management or climatic factors, etc.), and other questions. Whereas investigation of these questions would require literally years of experiments needing large amounts of resources, equipment, and trained personnel, properly calibrated models can allow for analysis of these items on a personal computer in a very short time. The implications of this tool for agricultural-water resources planning are substantial: computer models allow for the accumulation of the "experimental" results needed to derive crop-water production functions without the delay and expense of field experimentation and with an assurance of geographic portability since models can be calibrated to local environmental factors.

Most of the physiologically-based crop models in wide use today share their origins in a group of a few primary models. In fact, many crop models have been modified over the years so that particular components (e.g., water balance) are now shared among many different crop models.

Wilkerson et al.'s (1983) model of soybean growth, SOYGRO, was one of the first comprehensive physiologically-based crop models. SOYGRO included modules to consider a range of important states and processes in crop growth using a daily time step. The plant was modeled as having discrete organs (leaves, stems, shells, seeds, and roots), and dry matter content was considered each day in each organ as processes occur. Daily photosynthesis was computed as a function of daily radiation influx, leaf area, and factors relating reductions due to drought stress, temperature stress, and nutrient stress. Respiration of plant tissues was calculated and accounted for consumption of some photosynthetic carbohydrate product. Phenology (growth stage) was tracked and used to change partitioning fractions for allocating new carbohydrate to plant organs for growth. Growth characteristics of seeds were determined from accumulated quantities of growth and stresses during the season. Nitrogen dynamics within the plant were computed to determine possible stresses on growth and seed formation. A soil-plant water balance model was used to determine drought stresses. The model was calibrated and verified with field data and found to perform well.

Jones and Kiniry (1986) developed a simulation model for maize growth and development, CERES-Maize. The modeling philosophy for CERES-Maize was very similar to that of SOYGRO, although the independent development of these models resulted in different routines being used for many model components. CERES-Maize included the same basic sub-models as those listed above, and it also carried the capacity for the user to omit selected sub-models at his/her discretion. Since the advent of these two models, they have both been expanded to model other similar crops. SOYGRO was later modified to model peanuts, dry beans, and chickpeas, being legumes like soybeans, as well as tomato and pasture grass. CERES-Maize was expanded to simulate barley, millet, rice, sorghum, and wheat, all these crops being cereals. In addition to these two primary models and their progeny, several other crop models following similar modeling philosophy and methodology have been produced. These include the SUBSTOR-Potato model (Griffin et al. 1993) and the GUMCAS cassava model (Matthews and Hunt 1994).

Before discussing further the models named above, it should be stated that other models based on crop physiological processes have been developed, some for the express purpose of understanding crop-water relationships. In fact, some of these models were later incorporated into the models named above. What sets the CERES, GRO, etc., models apart is their comprehensiveness and modularity. All of these models include explicit modeling components for soil water balance, crop phenology, photosynthesis, growth partitioning, nutrient dynamics, and other important processes. Some of the models include additional capacity to account for damage due to pests and diseases. Models formulated in this manner require extensive calibration both in development and application. Yet, the depth and breadth of issues considered allows great flexibility in scenarios that may be simulated due to climatic, management, genetic, and geographic factors. Results obtained for simulations in one location may be directly compared to simulations for another location. This ease of transferability is lacking in other crop models such as the crop yield-ET model described in the previous section.

The comprehensive physiologically-based crop models named above have all been collected into a common pool for development. Under the aegis of the International Benchmark Sites Network for Agrotechnology Transfer (IBSNAT) and its successor the International Consortium for Agricultural Systems Application (ICASA), development of physiologically-based crop models has continued. IBSNAT/ICASA has standardized many of the routines among various models (e.g., soil water balance) and grouped several crop models and ancillary utility software into the Decision Support System for Agrotechnology Transfer (DSSAT) (Tsuji et al. 1994). The DSSAT is the state-of-the-science in agronomic simulation methods and can be used as an important tool in singular scale analysis.

3.2. Model Structure

The fundamental processes simulated by the DSSAT models on a daily basis (see Figure 4) include water balance, photosynthetic production, allocation of carbohydrate among plant organs, growth, phenological development, nitrogen uptake by the plant, nitrogen transport in the soil, and damage due to disease and pests. It is possible to omit some of these processes for a given simulation if they are not of interest. For example, irrigation planning simulations may be run where nutrient and fertilizer processes are assumed not to be limiting and are omitted. A discussion of model theory and operations is given below, but longer expositions can also be found in Jones and Kiniry (1986), Wilkerson et al. (1983), and the volume edited by Tsuji et al. (1998).

3.2.1. Plant Organs

The plants that are cultivated for human needs are highly evolved organisms with hundreds and thousands of individualized structures. It is practically impossible to attempt to model all of these structures at their real level of detail. Thus, crop models treat plants as being composed of a specific number of organs, and the number varies from crop to crop. Virtually all crop models include the following organs: roots, leaves, stems, and grain (a.k.a., seed or tuber). Beyond these four basic organs, individual crops may or may not include other important structures. Some examples include: ear (maize), shell (soybeans and peanuts), panicle (millet), and seed (potato, cassava, others).

Each organ then is treated in the model as being a single container of one or more substances. Primarily, the model tracks each organ by its quantity of carbohydrate biomass. That is, at any point in the simulation period if we look into the model and ask, "How many leaves are on the plant?", the first answer that we'll get back is, "There is 1402.65 kg leaf biomass per hectare of cultivated land." The same type of answer exists for roots, stems, grain, etc. Some crop models also track other substances in the "reservoir" of each plant organ. Nitrogen is the most common of these secondary components to be accounted for. Beyond the formulation of each organ as a biomass reservoir, some organs are also described in other morphological quantities; examples include: leaves (quantified in terms of leaf area per plant and leaf area per ground area,

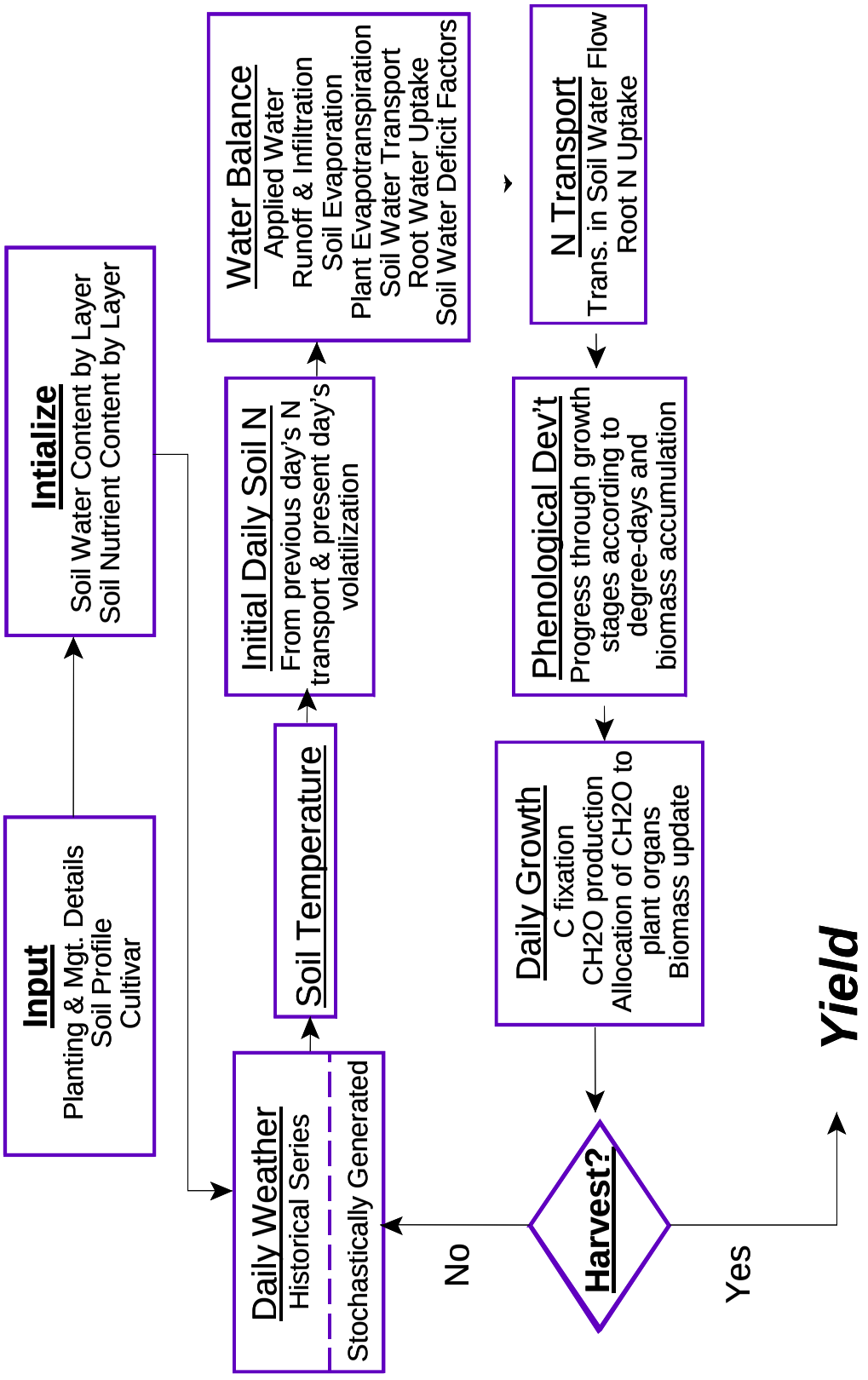

Figure 4. General Simulation Algorithm for Physiologically Base Crop Models

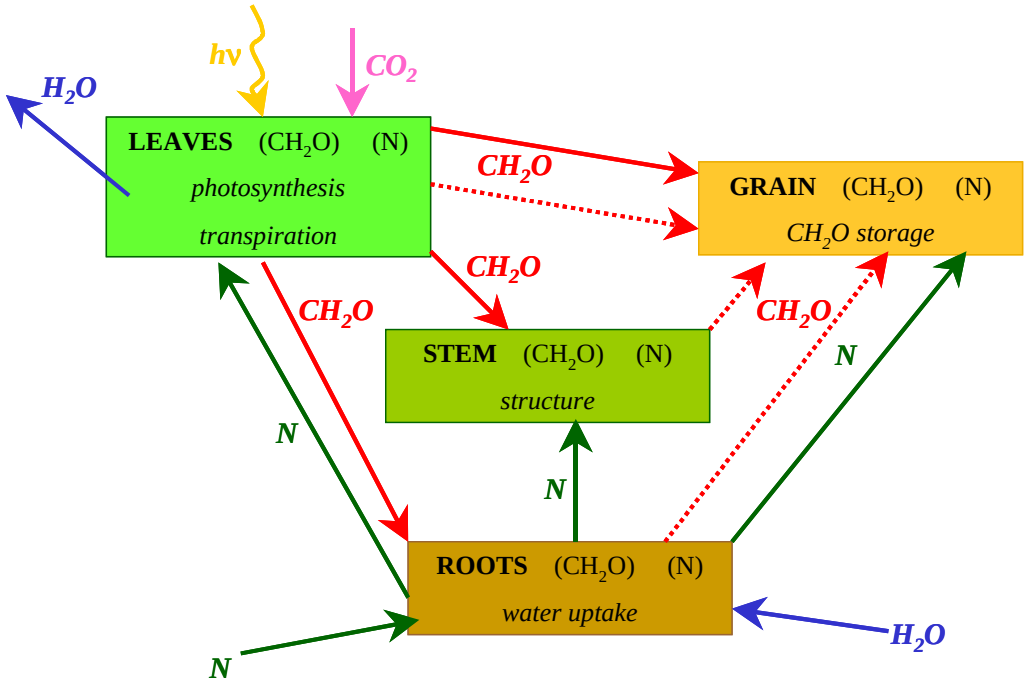

Figure 5. Conceptual Schematic of Plant Organ Structure in Crop Models

"LAI"; leaf number (i.e., order of emergence of leaves) is used in some models), roots (root length density is quantified for each soil layer; maximum rooting depth is calculated), and grain (number of grains per plant and grains per ear are frequently used). Figure 5 shows the conceptual manner in which plant structure is included in the model. The organs act as reservoirs with fluxes of material between various organs.

3.2.2. Phenology

Phenology is the progression of the plant through various stages of growth. Each phenological stage is marked by differing priorities of growth, organ formation, nutrient storage, and tissue senescence (death due to age). Again, every crop has its own phenological progression, and some experts will even disagree on the number of unique stages that a particular crop has. But, there are two general frameworks that most crops can be said to follow. Seed bearing crops (e.g., maize, wheat, rice, soybeans, etc.) follow a life cycle that is aimed toward maximizing the probability of the survival of a particular plant's genes to the next generation. These plants follow a general phenology which includes:

- Germination: A seed enters the ground and waits for acceptable conditions of ground temperature and soil moisture. When these conditions are met, the seed germinates and sends out a root and shoot. Energy requirements during this period are met by stored carbohydrate in the seed.

- Emergence: The shoot emerges from the ground surface and forms itself into a first leaf so that photosynthesis can begin, hopefully before the

seed's carbohydrate reserves are exhausted. Priorities in this stage are growth of leaves and roots to establish the fundamental machinery of water and nutrient uptake and carbohydrate production.

- Final structural building: The plant now grows a stem so that a larger leaf structure can be supported. Leaves continue to grow at a high rate that slows towards the end of the stage when maximum leaf area is reached. Roots are still growing, but they are less of a priority than before.

- Flowering: The plant produces flowers, and the success of their pollination rate directly determines the number of seeds to be produced. Leaf growth has ceased. Stem and root growth may continue at diminished rates.

- Seed production: The plant is now devoting all its resources to producing seeds. The great majority, if not all, of photosynthetic production goes directly to be stored in the seeds. Roots and stems are either growing very slowly or not at all. Most plants actually pull biomass out of the leaves, stems, and roots to be transferred to the seeds.

- Maturation: Taking its cue from some source (e.g., daylength, temperature, seed size, exhaustion of leaf biomass, etc.) the plant determines that it should shut down. Its seeds are then available to start the cycle in the next generation.

Starch-reserve bearing crops (e.g., potato, cassava) follow a life cycle not as definitely defined as seed bearing crops. While many of these plants also flower and produce seeds, they often do not die after seed production and can live through many reproduction cycles. Moreover, their agriculturally important feature is not their seeds but their tubers or corms, which are starch-reserve organs attached to the roots. It is more inexact to describe a general phenology for these crops, but it would be something like the following:

- Planting: These plants are typically planted as a "seed piece" of tuber or corm. The seed piece sends out roots and shoot, and their rate of growth is affected by soil temperature and moisture. Starch in the seed piece is the carbohydrate source driving the process.

- Emergence: Similar to the seed bearing plants. Root and leaf growth are priorities so that photosynthesis and uptake of water and nutrients can function.

- Structure building: This stage can last for very long periods and be quite variable in duration, which is different from seed bearing plants' more fixed durations in this stage. Another major difference is that excess photosynthetic product may be stored in tubers already at this stage, but the tubers can also be tapped during stressful periods.

- Structural maturity: The plant may reach a final size and enter a period of maintenance with excess photosynthate being stored in the reserve organ.

- Harvest: Actually determined by human decision to harvest the starch reserve. There is often no physiologically mandated end to the plant's life.

Phenology is most heavily influenced by two factors. First, "thermal time" is the product of time and air temperature and is the principal "counter" on the phenological "clock." Plants growing in warm environments tend to move more quickly through their growth stages than plants growing in cooler temperatures. Crop models keep a running tally of accumulated thermal time, and most growth stages are commenced upon the accrual of a specific number of degree-days. Genetic differences are the other key factor. Some varieties of crops are suited to constant temperatures throughout the growing season and have their "degree-day clocks" tuned to that environment. Other crops are heavily dependent on changes in daylength to trigger phenological stages.

The importance of understanding phenology for agricultural water resources planning is to have an appreciation for how and why plants need water at various times. For example:

- Soil must be moist for seeds to germinate but only in the zone immediately around the seed. While some irrigation might be necessary at planting, very deep watering may not be appropriate.

- The flowering period is critical for seed formation, so drought stress in this period is especially damaging.

- The seed formation period is also critical for final yield, but drought stress is less important towards the end of the plant's life. Irrigation in the last few days may have little value.

- Starch-reserve crops may benefit from avoidance of drought close to harvest but only if other conditions for photosynthesis are good.

3.2.3. Photosynthesis and Growth

Photosynthesis is the chemical process conducted in the leaves by which CO_2 and H_2O react in the presence of chlorophyll and solar radiation to produce carbohydrate CH_2O and O_2. Since carbohydrate is both the energy source and physical building block for the plant, photosynthetic production is essential for the plant to grow and produce a useful yield. The general process by which photosynthesis is modeled in the DSSAT models is as follows. The value of daily sunlight hours is converted to incoming solar radiation (MJ/m2) using the location's latitude and the day of the year. Next, total incoming radiation is multiplied by 0.5 to determine "photosynthetically active radiation"

(PAR), which is that portion of the total solar spectrum that chlorophyll actually absorbs and uses. Potential non-stressed carbohydrate production CH_2O_{pot} is computed as:

$$CH_2O_{pot} = \frac{\eta_{photo,crop} \cdot PAR \cdot \left(1 - \exp(-k_{LAI,crop} \cdot LAI)\right)}{N_{plants}} \quad \textbf{(10)}$$

where $\eta_{photo,crop}$ is crop-specific photosynthetic efficiency (5 g CH2O/MJ PAR for maize, 3.5 g CH2O/MJ PAR for wheat, etc.), $k_{LAI,crop}$ is a crop-specific coefficient whereby leaf interception of PAR follows Beer's Law (0.65 for maize, 0.85 for wheat, etc.), and N_{plants} is the number of plants per square meter of ground. If the plant is undergoing drought, temperature, or nitrogen stress, actual carbohydrate production is reduced by the most stressful factor:

$$CH_2O_{actual} = CH_2O_{pot} \cdot \min\left[SWDF_P, TSF, NSF\right] \quad \textbf{(11)}$$

where $SWDF_P$ is the photosynthesis soil water deficit factor discussed below in section 3.2.4, and TSF and NSF are temperature and nitrogen stress factors, respectively. Each factor varies from 1 (no stress) to 0 (extreme stress).

From these equations follow some important observations for agricultural and water resources planning. First, as solar radiation is a direct input into the photosynthesis model, the time-series of sunshine hours input to the model must be as accurate as possible. Data limitations may require estimation or synthetic production of sunshine hours. Any bias in this estimation may force crop simulations to unrealistic and incorrect results. Second, a direct effect of drought stress on plant physiology is found in the possible reduction in CH_2O_{actual} due to $SWDF_P$. Since photosynthesis occurs every day after emergence, isolated drought stress episodes may not have much effect on crop yield. However, extended drought stress, especially during critical phenological stages such as flowering, can significantly harm eventual crop yield.

Each day's photosynthetic production CH_2O_{actual} forms the pool of new biomass material that can be used for new growth of plant organs that day. (In the germination and emergence stages, seed reserves may also be available). The process by which daily photosynthate is distributed to organs varies with phenological stage as explained earlier. Moreover, the processes are extremely complex and crop-specific.

3.2.4. Water Balance and Drought Stress Effects

A schematic of the water balance sub-model used in crop models in the Nile DST is shown in Figure 6. A complete exposition of the sub-model is given by Ritchie (1998). Daily water balance computations begin with the soil water content of each soil layer from the day before. If rainfall or irrigation occurs that day, the amount of precipitation becoming runoff is determined, and the remainder infiltrates into the top soil layer. Moisture transport between soil layers is calculated according to soil water

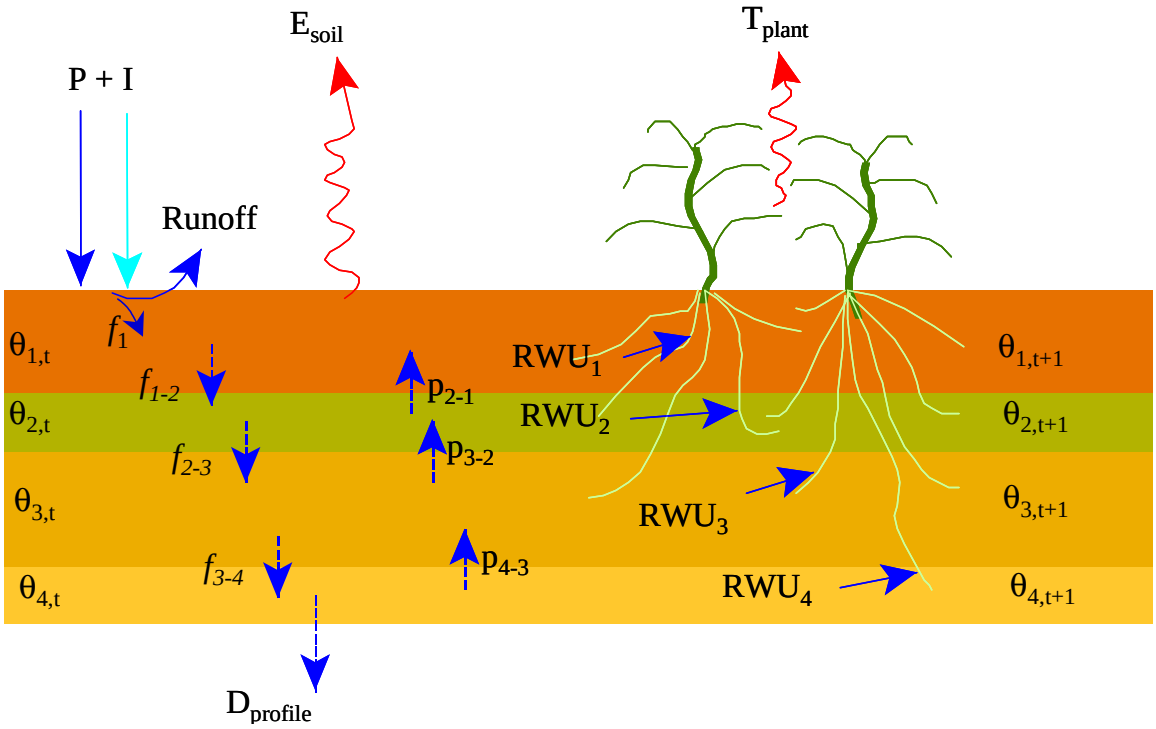

Figure 6. Schematic of Water Balance Sub-Model

differentials and an empirical transport coefficient analogous to hydraulic conductivity. Water draining out of the soil profile is calculated. Soil evaporation and plant transpiration are computed separately according to Ritchie (1972) and subtracted from the uppermost soil horizon. Evaporation from the surface layer of soil is determined according using the Penman equation. Transpiration from the plant is calculated as a function of PE and leaf area index. Root water uptake is found for each soil layer from root length in the layer and transpirative potential. If soil dryness necessitates that root water uptake be less than transpirative potential, a set of soil water deficit factors are computed which will serve to decrease growth and grain production for that day. Finally, soil water content for each layer is found for the end of the day to be referenced the next day. The soil water sub-model has been extensively tested and shown to perform well. Verification studies are included in Ritchie (1972), Gabrielle et al. (1995), and Brumbelow and Georgakakos (2001).

As mentioned above, a set of three "soil water deficit" (or "drought stress") factors are computed in the water balance sub-model. A more thorough discussion of how these factors affect crop growth and production is important. (Some of the equations below are parameterized for the maize model, but the general model processes are shared by all crop models in the Nile DST). The first factor affects root growth and will be referred to as $SWDF_R$ in this report. The second factor affects photosynthesis and will be referred to as $SWDF_P$. The third factor affects plant cell expansion and will be referred to as $SWDF_{CE}$. All three stress parameters can range from 0 to 1 (inclusive). Values of

unity indicate no stress; the factors are used as coefficients to reduce values of other processes under conditions of stress.

The root growth stress parameter $SWDF_R$ is computed for each soil horizon as a function of plant-extractable water in that horizon:

$$SWDF_R = \min\left(1,\ 4 \cdot \frac{\theta_l - \theta_{LL,l}}{\theta_{DUL,l} - \theta_{LL,l}}\right) \quad \textbf{(12)}$$

where θ_l is soil moisture content in soil layer l, $\theta_{LL,l}$ is the soil water lower limit for layer l, and $\theta_{DUL,l}$ is the soil water drained upper limit for layer l. Thus, $SWDF_R$ is equal to unity (meaning no effect on root growth) when plant-extractable water is at least 25% of the soil horizon's capacity. When soil moisture content in a horizon equals the lower limit (meaning no plant-extractable water is available), $SWDF_R$ equals zero and root growth in that layer is nil. The root growth stress parameter is the only one of the three factors computed directly from soil moisture contents.

The remaining drought stress parameters are calculated in a manner very similar to each other. Each is based upon the ratio of potential plant transpiration to root water uptake. In contrast to $SWDF_R$, which assumes independent values for each soil layer, $SWDF_P$ and $SWDF_{CE}$ each have a single quantification for the entire soil-plant-atmosphere-water system. The factors are expressed mathematically as:

$$SWDF_P = \min\left(1,\ \frac{\sum_l RWU_l}{T_{pot}}\right) \quad \textbf{(13)}$$

$$SWDF_{CE} = \min\left(1,\ 0.67 \cdot \frac{\sum_l RWU_l}{T_{pot}}\right) \quad \textbf{(14)}$$

where RWU_l is root water uptake in soil layer l, and T_{pot} is potential transpiration. Root water uptake in each soil horizon is computed as a function of plant-extractable soil water and root length content in that horizon:

$$RWU_l = 0.00267 \cdot \exp\left(\frac{62 \cdot \left(\theta_l - \theta_{LL,l}\right)}{6.68 - \ln\left(RLV_l\right)}\right) \quad \textbf{(15)}$$

where RLV_l is root length per soil volume (e.g., units of centimeter of roots per cubic centimeter of soil). Potential transpiration is computed as a function of potential evapotranspiration ET_{pot} (calculated by the Penman or Priestly-Taylor equations), leaf area index LAI, and evaporation from the soil alone $E_{soil,pot}$ (the water balance sub-model uses the decoupled soil evaporation-plant transpiration model of Ritchie 1972):

$$T_{pot} = \begin{cases} \min\left(ET_{pot} \cdot \dfrac{LAI}{3}, \quad ET_{pot} - E_{soil,pot} \right) & , if\ LAI < 3 \\ ET_{pot} - E_{soil,pot} & , if\ LAI \geq 3 \end{cases} \quad \textbf{(16)}$$

Thus, the drought stress indices affecting photosynthesis and cell expansion are functions of the ratio of potential water inflow to the plant (root water uptake) to potential water outflow from the plant (transpiration). When water inflow can not fully cover outflow, photosynthesis and actual transpiration are reduced by the plant water balance shortfall. That is, if potential root water uptake is 80% of potential transpiration, photosynthesis and actual transpiration will occur at 80% of their potential rates. Cell expansion is even more sensitive to moisture stress as it is decreased when potential root water uptake is less than 1.5 times potential transpiration. Thus, if potential root water uptake is 115% of potential transpiration, cell expansion (and some other growth processes explained later) is reduced to 77% of its potential rate.

The root growth soil water deficit factor restricts the growth of new roots in each soil horizon when soil water content is below 25% of the plant-extractable water capacity of the horizon (the difference between the drained upper limit and the lower limit). Total biomass available to produce new roots is calculated on a daily basis by the growth and carbohydrate partitioning sub-model. This potential new root biomass is computed according to a set of functions that vary according to phenological stage. Other factors influencing root growth in each soil layer are the layer thickness, the already existing density of root material, and the propensity of the soil layer for root growth (a characteristic of the soil input by the model user). The last factor is determined a priori according to empirical information and is related to the tendency for plant roots to be more common close to the surface and less dense as depth increases. The effect of $SWDF_R$ is to reduce actual new root growth in a particular soil layer below the potential growth according to soil dryness. For example, if a particular soil layer has θ_{LL} = 0.200, θ_{DUL} = 0.300, and θ = 0.210, plant-extractable water capacity is 0.100, and available plant-extractable water is 0.010 or 10% of capacity. In that case, $SWDF_R$ would be 0.40, and root growth in this soil layer for that day would be reduced by 60% from the potential growth as determined by partitioned biomass, soil layer thickness, pre-existing roots, and the soil layer propensity for root growth.

The photosynthesis soil water deficit factor directly affects three unique processes. First, since $SWDF_P$ is the ratio between potential root water uptake and potential transpiration, for simulation days where the former is insufficient to meet the latter, actual transpiration is reduced from its potential value in accordance with the value of $SWDF_P$. This adjustment is necessary to ensure proper mass balance for the plant.

Second, for all growth stages $SWDF_P$ acts as a control on daily photosynthetic production of new carbohydrate. Potential photosynthetic production $(CH_2O)_{pot}$ is modeled as (some coefficients here are specific to maize):

$$(CH_2O)_{pot} = 5 \cdot \left(0.02 \cdot R_{s,plant}\right) \cdot \left[1 - \exp(-0.65 \cdot LAI)\right] \quad \textbf{(17)}$$

where $R_{s,plant}$ is incoming solar radiation per plant, the coefficient *0.02* accounts for the fraction of total radiation that is photosynthetically active, and *LAI* is leaf area index. The potential daily carbohydrate production is then potentially reduced by the most significant of three stress factors, one each for adverse temperature, nitrogen deficiency, and drought:

$$(CH_2O)_{act} = (CH_2O)_{pot} \cdot \min\left(TSF, NSF, SWDF_P\right) \quad \textbf{(18)}$$

where *TSF* is an adverse temperature stress factor and *NSF* is a nitrogen deficiency stress factor. Thus, assuming that temperature and nitrogen stresses are not more important than drought stress, the lack of available soil water diagnosed by $SWDF_P$ controls that day's photosynthetic production of carbohydrate, which is the basis for all new plant growth for that day.

Third, $SWDF_P$ acts as a control on grain biomass growth during the grain filling stage of the plant's life cycle. During the grain filling stage, daily grain biomass growth ΔB_G is modeled as (again using maize model coefficients):

$$\Delta B_G = R_{gf} \cdot GPP \cdot G_3 \cdot 0.001 \cdot \left(0.45 + 0.55 \cdot SWDF_P\right) \quad \textbf{(19)}$$

where R_{gf} is a zero-to-unity rate of grain fill determined on a daily basis according to daily air temperature, *GPP* is the number of grains per plant which is determined at the end of the previous phenological stage by a genetic parameter and the cumulative photosynthetic production during that phenological stage (note the dependence of *GPP* on $SWDF_P$ values in this stage), and G_3 is a genetic parameter. Thus, grain growth is affected by $SWDF_P$ in two ways: indirectly through the establishment of the number of grains per plant in the post-silking growth stage, and directly during the grain filling period by a linear relationship allowing reductions of up to 55%.

The cell expansion moisture stress index $SWDF_{CE}$ directly affects the growth rates of all plant organs except the grain, which is indirectly affected due to various feedback mechanisms. In the early growth stages when leaves are growing (leaf growth stops at mid-season), $SWDF_{CE}$ is a direct coefficient on daily growth of leaf area per plant ΔLA_{plant}. The exact function to compute ΔLA_{plant} varies by crop, growth stage, and number of leaves emerged. One specific case of the function is for the first growth stage of maize (plant emergence to end of juvenile stage or seed reserve exhaustion) with greater than four leaves emerged:

$$\Delta LA_{plant} = 3.5 \cdot \left(L_{num}\right)^2 \cdot \frac{DTT}{38.9} \cdot SWDF_{CE} \quad \textbf{(20)}$$

where L_{num} is the number of leaves emerged and *DTT* is daily thermal time, the product of time and temperature relative to a base temperature. In growth stages 1 and 2, biomass available for root growth is equal to the remaining daily carbohydrate production after that used for new leaf biomass is subtracted. Thus, during periods of $SWDF_{CE}$ values less than unity, the plant experiences a growth preference towards new roots as opposed to new leaf area. This adaptive growth pattern is logical in that it would subsequently increase root water uptake capacity and hold transpirative capacity (as a function of leaf area) steady. Ritchie (1998) reports that this phenomenon is a "common experimental observation." Similar feedback effects on root growth occur throughout the plant growth cycle.

Stem growth in maize occurs during phenological stages 3 and 4 and is directly affected by $SWDF_{CE}$. Like the leaf growth model, stem growth functions vary with growth stage and number of emerged leaves, but one example of the stem growth function is for growth stage 4:

$$\Delta B_S = 0.088 \cdot DTT \cdot SWDF_{CE} \quad \textbf{(21)}$$

where ΔB_S is daily change in stem biomass. Ear growth in maize occurs only in growth stage 4. The function determining daily new ear biomass ΔB_E is:

$$\Delta B_E = 0.22 \cdot DTT \cdot SWDF_{CE} \quad \textbf{(22)}$$

3.3. Crop Models Included in the Nile DST

The Nile DST includes the crop models of the Decision Support System for Agrotechnology Transfer (DSSAT). These crop models were chosen for their technical superiority, verification track-record, and amenability to incorporation in advanced irrigation planning methods. The specific crops included in the Nile DST are:

- Maize,
- Wheat,
- Millet,
- Sorghum,
- Barley,
- Rice,
- Cassava,
- Potato,
- Peanut (Groundnut),
- Dry Bean, and
- Soybean.

The Rice model is included in two forms: one for flooded paddy cultivation, and one for upland cultivation. The paddy rice model includes only a simple paddy irrigation scheduler based on soil infiltration rates and flood timing, and a single yield-irrigation point is determined. All other crops can be used with the CWPF determination methods described in Section 4.

Irrigation scheduling according to the CROPWAT program is also available in the Nile DST Agricultural Planning module. As discussed above, this option will produce only a single yield-irrigation point, not a full CWPF. Irrigation schedules can be determined with or without the soil water balance routines. (Cassava has not been included in published versions of CROPWAT, so it can not be modeled with CROPWAT in the Nile DST.

3.4. Model Input and Output

Input data to the DSSAT models generally fall into three broad categories. First, meteorological data are needed on a daily basis and include: incoming solar radiation or hours of sunshine per day, maximum and minimum air temperatures, rainfall, windspeed, and relative humidity. In the Nile DST, meteorological data is gathered from the Database module of the software. The Nile DST User Manual should be consulted for specific instructions on selection of meteorological data for Agricultural Planning analyses. The module does employ a method of data estimation for days where specific parameter values are unavailable. This method makes use of a climatological zone database generated from the station data in the Nile DST database (see Figure 7). The climate zone database treats each country as a zone. In the case of Sudan, there are three zones: Sudan Northeast, Sudan Northwest, and Sudan Southern. Sudan was split into three zones as there are three distinct climatic areas in Sudan, the Sudd, the desert, and the Blue Nile portion. For each day in the year, all data available within a zone is averaged into a single, representative value. The result is a 365 day time series of values for each of the meteorological parameters used in the agricultural planning module other than precipitation. When the user builds a planting location and specifies a year, the interface first uses any data available for the specified station. If no data is available, then data from the climate zone database is used.

The second class of data needed for Agricultural Planning simulations is geographical data. This includes soils and topography. Soil data is input as a soil profile divided into horizons based upon differences in texture, nutrient content, and other factors. For each horizon, data is required on layer thickness, composition (sand/silt/clay), density, carbon and nitrogen content, pH, permeability, hydraulic conductivity, and root abundance. Topographic data include elevation and latitude of each planting location. All geographic data is gathered from the GIS database of the Nile DST.

The third category of model input is information on the crop, management, and planting details: crop and crop genotype, planting date, and irrigation scheduling

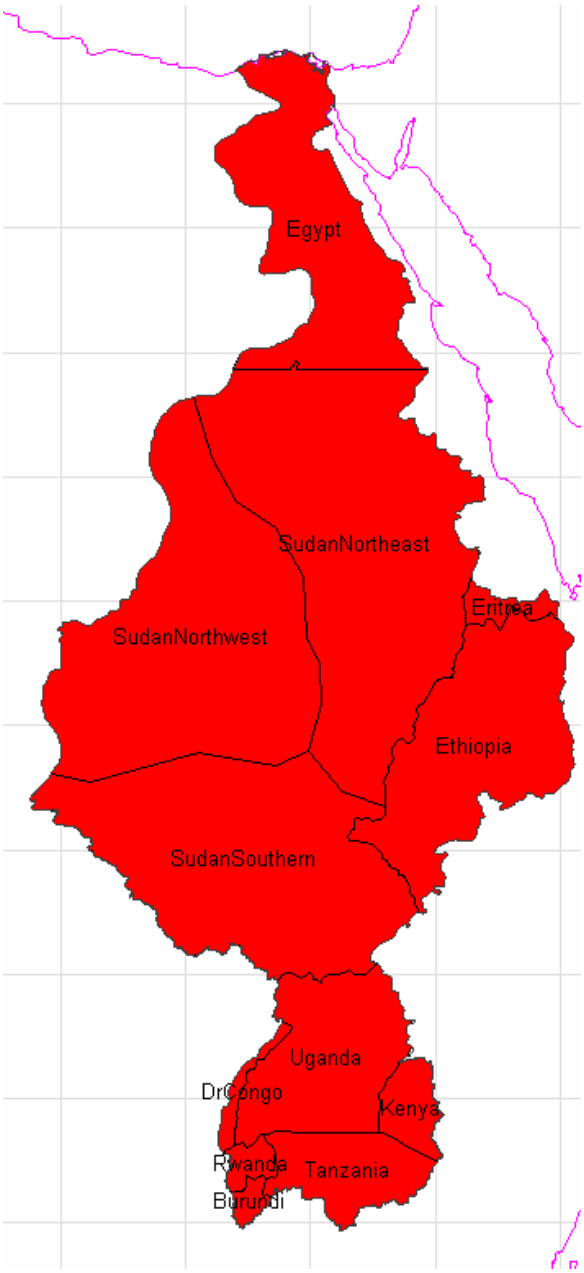

Figure 7. Climatological Zones Used in Nile DST Database and Agricultural Planning Modules

preference. The system uses default values for some options if the user does not wish to specify them. Again, the User Manual should be consulted for details.

Model outputs include a variety of water and biophysical quantities. Most of these are available as time-series across the full growing season. The principle outputs for purposes of agricultural water resources planning are the CWPF and the irrigation schedules corresponding to points on the CWPF. However, examination of outputs such

as drought stress indices, biomass, and leaf area index can give a user insight into how the modeled crop responds to changes in irrigation and various climatic forcings.

3.5. Model Verification

The DSSAT has been developed for and continues to be refined by a diverse, global group of investigators. As such, improvements in both capability and accuracy are continually being made. Verification data are included in most of the reports describing model developments that have been mentioned above. Garrison et al. (1999) verified the performance of the water and nitrogen balance components of the models under tile-drained conditions. Roman-Paoli et al. (2000) have investigated the accuracy of genetic parameter evaluation. Alagarswamy et al. (2000) have verified the performance of the DSSAT soybean model for vertic inceptisol soils. The DSSAT crop models have been used both as tools to study irrigation effects on crop systems and as tools for prescription of irrigation scheduling (e.g., Steele et al. 1994). The soil water sub-model has been extensively tested and shown to perform well. Verification studies are included in Ritchie (1972), Jones et al. (1980), Gabrielle et al. (1995), and Brumbelow and Georgakakos (2001). Results of two verification studies of the DSSAT maize model are shown in Figures 8 and 9. The first graph is from the original verification studies of the model (Jones and Kiniry 1986) and shows measured versus simulated crop yield for 37 different experiments. The second figure is a comparison of measured versus simulated maize yields for experiments at the Namulonge, Uganda, agricultural experiment station. These results are typical of the other verification studies cited above.

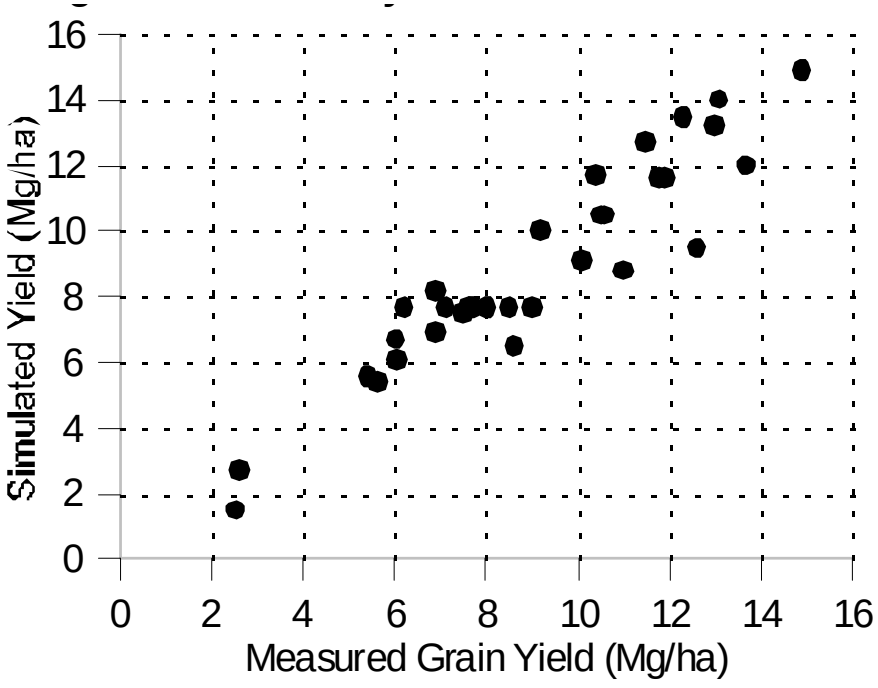

Figure 8. Verification Study Results for Maize Model Crop Yield (after Jones and Kiniry 1986)

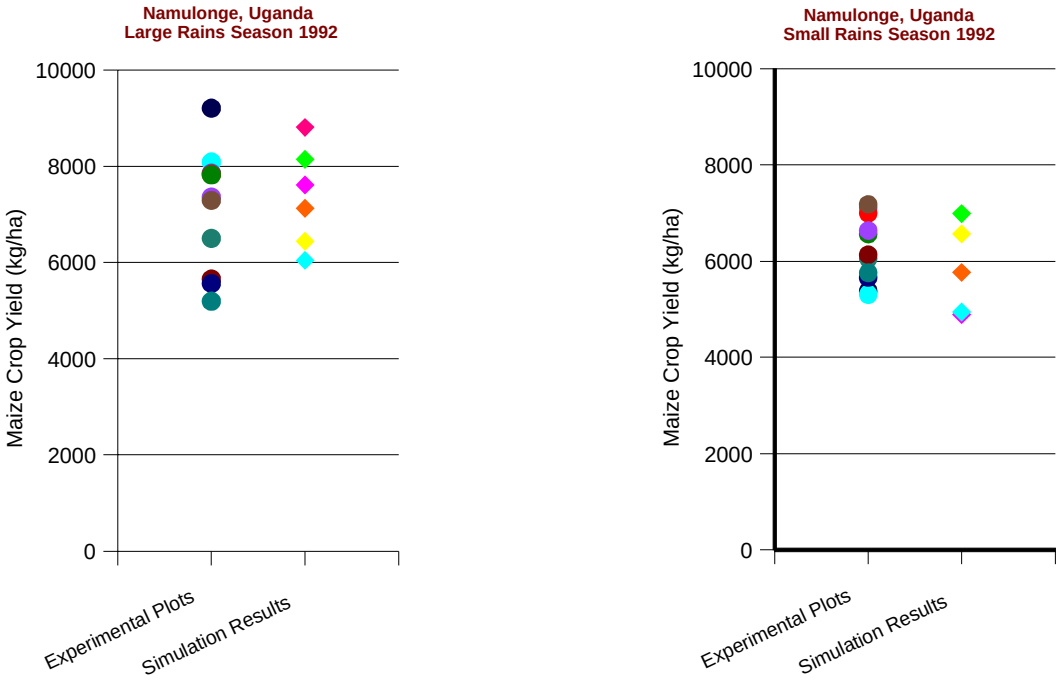

Figure 9. Comparison of Maize Yields Measured and Simulated at Namulonge, Uganda

4. Irrigation Planning Algorithms

The Nile DST Agricultural Planning module includes several algorithms for determination of CWPF's for purposes of irrigation planning. This section describes the development and operation of these algorithms. As will be discussed, the various methods represent a range of optimality of results and computational resource requirements, and a definite tradeoff exists. Better results require more computer time. In addition, the two main categories represent fundamentally different means by which to schedule irrigation, and these vary in intuitiveness. The Moisture Stress Threshold method is more easily understood and reflects common perceptions of how crops grow. However, the Yield-Irrigation Gradient methods usually produce more optimal results. Again, the tradeoff exists, and the user should evaluate his or her preferences among the options available.

Sections 4.1 and 4.2 below describe the general theory and implementation of the algorithms. Case studies of application of the algorithms to Nile Basin sites are given in Section 5.

4.1. Moisture Stress Threshold (MST)

The existence of moisture stress indices in physiologically-based crop models leads to a query as to how they may be used to assist irrigation planning. Since these parameters diagnose periods of low soil moisture uptake and are used to calculate physiological effects on growth, their value is unquestionable. This section presents a methodology and implementation by which a modeled physiological drought stress index is used to assist in planning of irrigation.

The drought stress indices calculated in physiologically-based crop models indicate periods where insufficient soil moisture uptake results in impaired plant growth processes. The technique developed here requires the user to choose a moisture stress threshold (MST) at which he or she desires irrigation to be applied to mitigate drought effects. The MST method is flexible in that it is independent of crop type, soil, irrigation application frequency, and other factors.

Of the three drought stress factors discussed above, $SWDF_{CE}$ is used as the MST method's sole drought stress indicator. This choice is due to several factors. First, $SWDF_{CE}$ has the largest number of direct and indirect effects on crop growth. As discussed above, $SWDF_{CE}$ is included in carbohydrate partitioning and computation of biomass growth for all plant organs, whereas $SWDF_R$ only affects root growth, and $SWDF_P$ only directly factors into partitioning for grain. Second, the obvious correlation between $SWDF_P$ and $SWDF_{CE}$ and the higher sensitivity of $SWDF_{CE}$ means that any phenomena captured by $SWDF_P$ values is also captured by $SWDF_{CE}$ values. Third, while the derivation of $SWDF_R$ from soil moisture values appears to be independent from the plant water balance consideration that produces $SWDF_{CE}$, it is likely that any period having soil moisture low enough to produce stress measurable by $SWDF_R$ will also

produce stress measurable by $SWDF_{CE}$. Thus, $SWDF_{CE}$ is seen to be the most sensitive and far-reaching of the three indices.

Most irrigation application in the field occurs with water being applied at discrete intervals; applications by drip-irrigation and flood irrigation are exceptions where water can easily be applied continuously. Therefore, it is logical to observe moisture stress quantities as aggregates over these discrete intervals. The question of how to aggregate drought stress values over time then arises. Possibilities for aggregation include summation, maximum values, duration above no stress, and others. Of these possibilities, summation of moisture stress values is the best choice. The drought effects on growth listed above accumulate over the season to produce reduced yields. Means of drought stress may minimize reduced growth effects for long irrigation intervals. Maximum values would ignore all lesser values during the same period. A duration criterion would not indicate drought severity. Judging among these possibilities, summation represents the best aggregation of the drought stress indicator over time as affecting eventual crop yield.

The principal components of the MST irrigation planning method are thus defined: $SWDF_{CE}$ is the drought stress indicator, the MST user defines acceptable stress levels during each irrigation interval, and summations of daily moisture stress values over the irrigation interval are compared to the MST to determine the need for and quantity of irrigation to apply. The implementation of the MST method follows (see Figure 10a-e):

1) The daily moisture stress statistic ms_d is redefined from daily $SWDF_{CE}$ as:

$$ms_d = 1 - SWDF_{CE,d} \quad \textbf{(23)}$$

so that it equals zero to indicate no stress and equals unity at complete moisture stress (i.e., no root water uptake).

2) Daily moisture stress ms_d is summed over all days in an irrigation interval to produce aggregate moisture stress MS for that interval:

$$MS = \sum_{d=1}^{n} ms_d \quad \textbf{(24)}$$

3) Step 2 is applied for all irrigation intervals in the growing season.

4) Starting from the first irrigation interval, each interval's aggregate moisture stress value is compared to the user-defined allowable moisture stress threshold (MST) until an interval is found where moisture stress exceeds the MST.

5) Using some search method, the lowest irrigation application is found that reduces aggregate moisture stress below the MST for the interval in question. (Examples of search methods include simple upward incrementing from zero and interval halving).

6) Proceed forward through the growing season repeating steps 4 and 5 until all irrigation intervals have aggregate moisture stress below the MST.

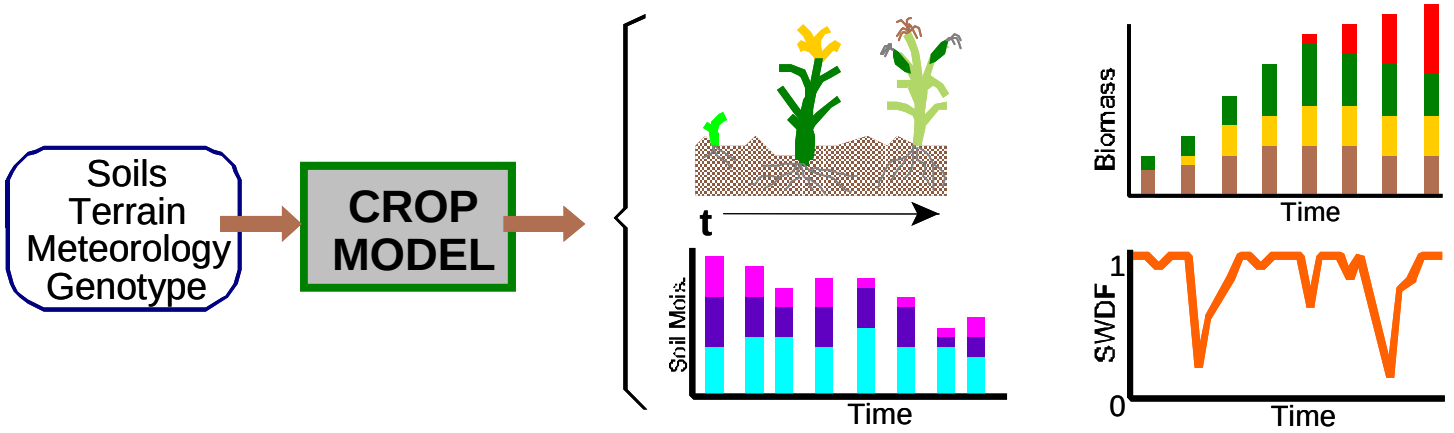

(a) Crop Growth is Simulated without Irrigation and Output Time-Series are Recorded

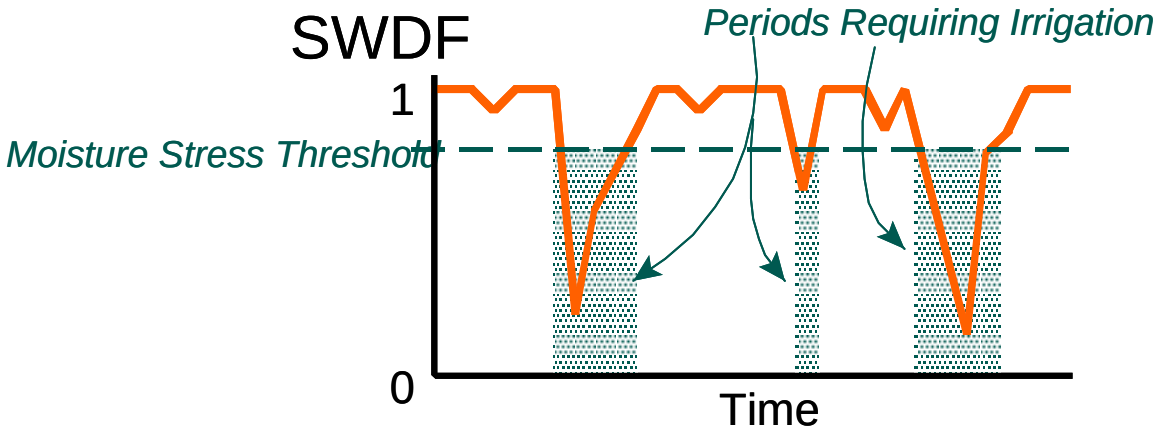

(b) Periods where Moisture Stress Crosses a Chosen Threshold are Identified as Needing Irrigation

Figure 10a-b. Implementation of the Moisture Stress Threshold Algorithm

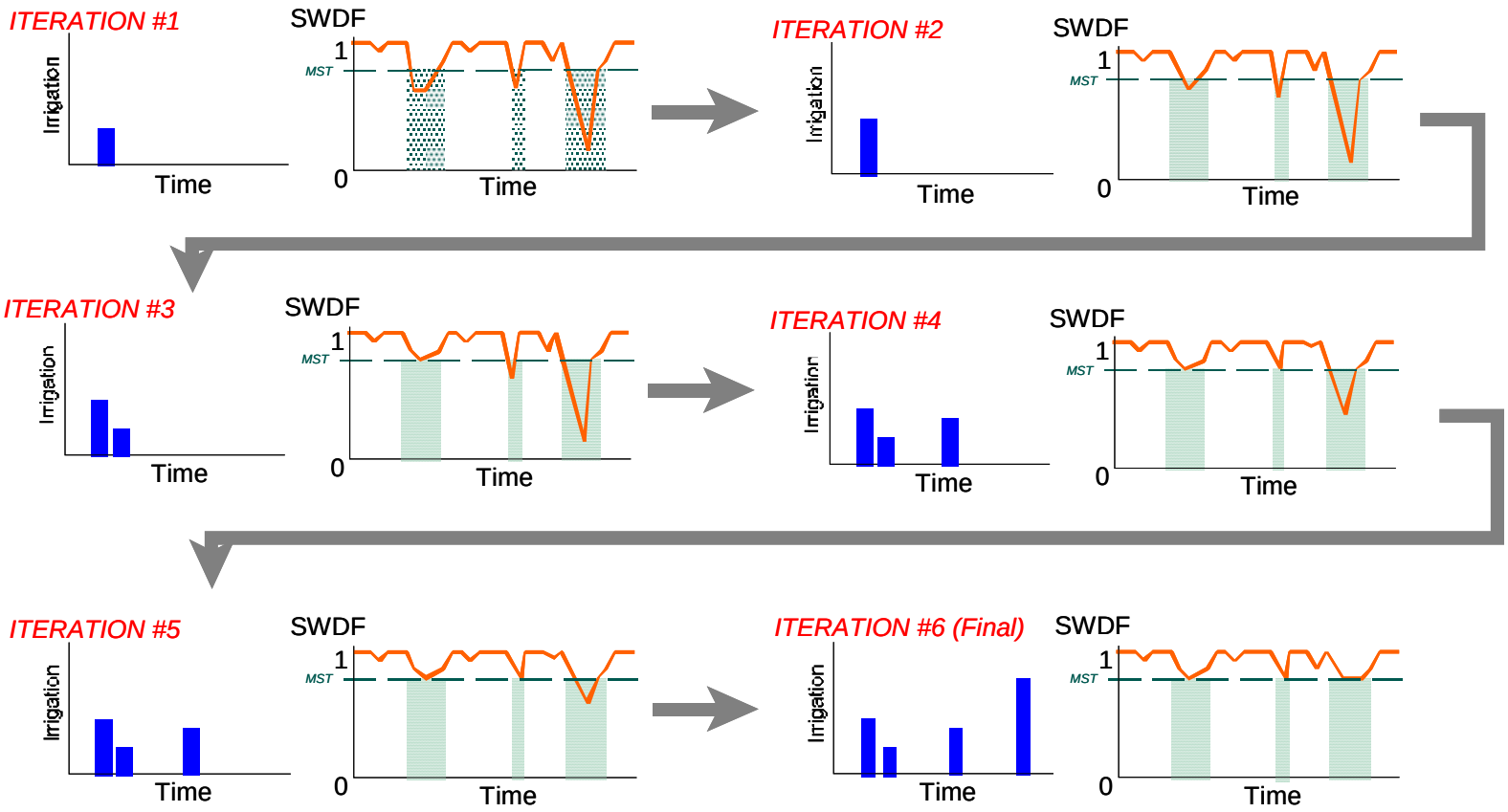

Figure 10c. Implementation of the Moisture Stress Threshold Algorithm

(c) Iterations are Made on Irrigation Schedule until All Periods Beyond Moisture Stress Threshold Have Been Eliminated

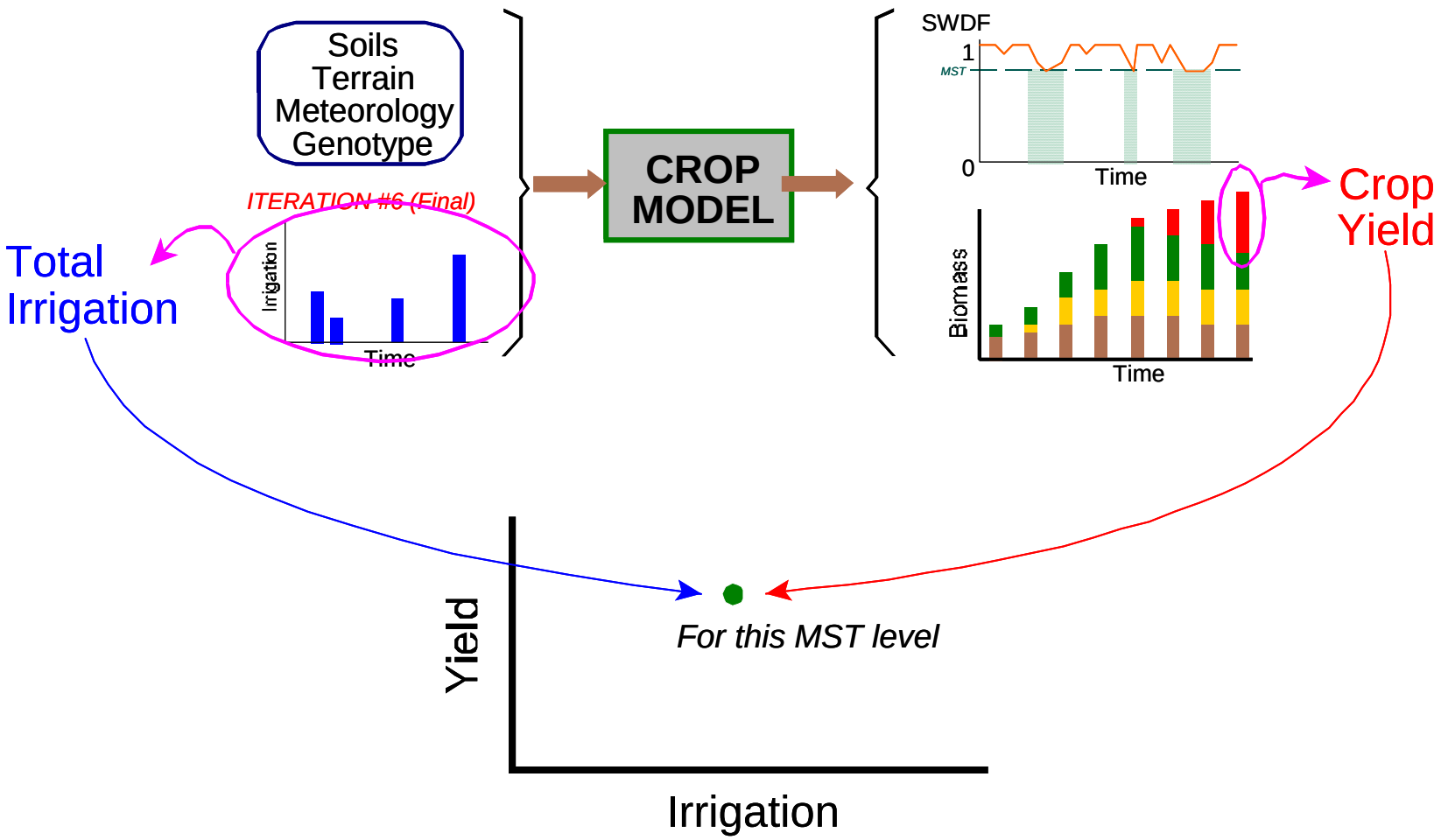

Figure 10d. Implementation of the Moisture Stress Threshold Algorithm

(d) Crop Model Simulation Results are Used to Determine One Point on the Crop-Water Production Function Corresponding to the Current MST Level

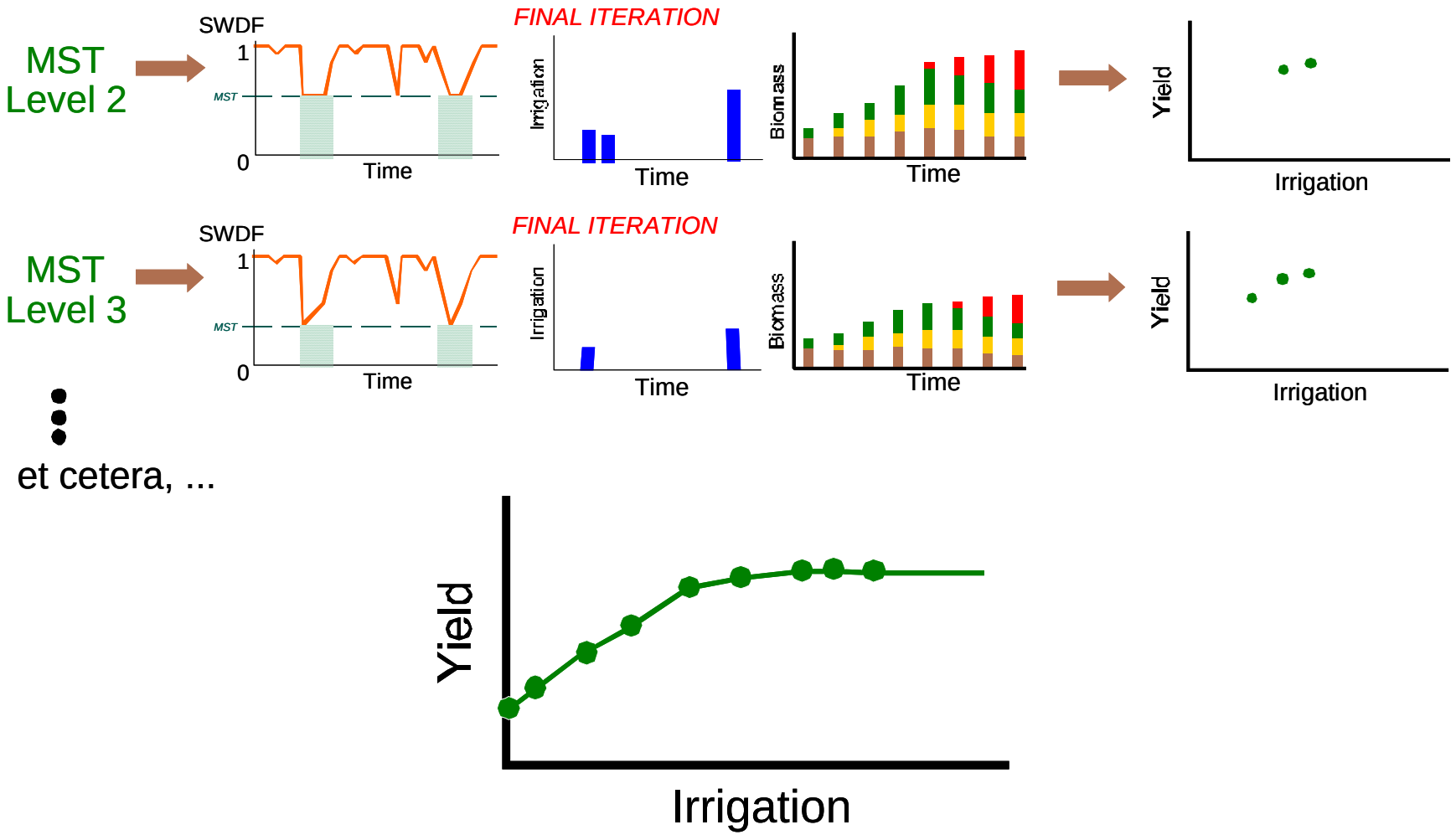

(e) Derivation of the Full Crop-Water Production Function by Irrigation Scheduling at Various MST Levels

Figure 10e. Implementation of the Moisture Stress Threshold Algorithm

The implementation requires a progression from beginning to end of the growing season since the additional soil moisture introduced from irrigation applications will affect soil moisture contents in later time periods. This requirement, in addition to the need for continual evaluation of moisture stress values in response to changing irrigation amounts, mandates that the crop model be operated repeatedly. The number of model simulation runs required to produce a final irrigation schedule will be one criterion by which to judge the performance of the irrigation planning methods and various parameterizations of those methods presented in this report.

The MST irrigation planning method provides a means by which to derive crop-water production functions. The user-defined *MST* value can vary continuously from zero, where crop yield is at its non-water-limited optimum, to a maximum (equal to 1.0 times the number of days in an irrigation interval), where no irrigation is applied and crop yield is at its rainfed value. By calling on the MST method to produce irrigation schedules for a range of *MST* values from minimum to maximum, a series of yield-versus-irrigation pairs are produced which corporately form a crop-water production function. Examples of this process will be given in the Section 5. The optimality of crop-water production functions produced by the MST method also will be assessed.

Specific values of the *MST* parameter may also be seen as indicative of field management preferences. Brumbelow and Georgakakos (2001) modeled regional crop production across the United States including undetermined mixtures of irrigated and non-irrigated acreage by calibrating *MST* values so that modeled yields matched historically observed yields. The local calibrated *MST* values matched expectations with western U.S. areas having low threshold values consistent with the dependence of virtually all crop production in these areas on irrigation and eastern U.S. areas having higher thresholds in line with the scattered use of irrigation.

As implemented in the Nile DST, CWPF's generated by the MST algorithm have 51 points corresponding to 10-day stress thresholds of 0 to 10 incremented by 0.2. The length of each irrigation period is 10 days.

4.2. Yield-Irrigation Gradient (YIG)

While the MST method is intuitive and can approximate the natural inclinations of irrigators, it is not necessarily an optimization method. As will be seen in examples below, the CWPF's produced by MST tend to be sub-optimal. That is, one can alter an irrigation schedule produced by MST for a given seasonal irrigation amount and produce higher crop yield. The desire for a true optimization technique that can work in conjunction with advanced, physiologically based crop models has led to development of the Yield-Irrigation Gradient (YIG) techniques. These methods can achieve maximum possible crop yields for a given seasonal irrigation total. A new set of techniques has been necessary because of the incompatibility of traditional optimization techniques with crop models. The crop models' complexity makes the use of traditional optimization techniques quite difficult. For example, linear programming (LP) application would be

stalled by the fact that most state dynamics in recent crop models are highly non-linear. The traditional means to overcome this problem is to approximate non-linear dynamics as being "piecewise linear," consisting of linear segments across the appropriate domain that collectively approximate the original function. However, the sheer number of dynamical elements to consider makes that process extremely difficult. Another traditional optimization technique is dynamic programming (DP), which is insensitive to non-linearity in state dynamics. DP requires that large numbers of possible state transitions, control decisions, and performance values be stored as the algorithm searches for an optimal solution. When systems include large numbers of state variables and many stages over which to consider control sequences, this "curse of dimensionality" can easily overwhelm computational resources. The soil-plant-atmosphere-water system of physiologically-based crop models easily fits into the category of systems able to overwhelm DP implementation. A proper DP implementation would include one state variable for each of the four biomass components, one state variable for each soil horizon moisture content, additional state variables for important physiological quantities (e.g., stage 4 carbohydrate production in the maize model), and at least one state variable for drought stress, among others. Assuming the inclusion of nine state variables, each discretized to ten levels, and a growing season of twenty irrigation periods, the DP implementation would require that 20 billion state transitions be considered. If each state transition required 0.01 seconds to simulate, the total computational time would be about 6.3 years. If the data storage for one state transition were approximately 500 bytes, a total of 10 terabytes of data storage would be required. Clearly, this computational overhead is prohibitive.

The optimal irrigation planning algorithm presented here fundamentally determines the value of irrigation allocations by the differential changes in crop yield that result from differential irrigation allocations. These yield-irrigation gradient (YIG) values are computed for each day in the growing season. The YIG value becomes a target for maximization as irrigation is added, and it is minimized as irrigation is deducted.

It is instructive to review the general form of the crop-water production function (Figure 11). If the optimal function is known, then for any seasonal irrigation quantity the function value for that irrigation corresponds to an irrigation schedule, not necessarily unique, that produces the highest yield possible for the given irrigation total. As viewed on a graph of yield versus irrigation, there exist no yield-irrigation pairs above or to the left of the crop-water production function. The function itself is the locus of optimal yield-irrigation pairs.

At any point of the function, the partial derivative of yield with respect to irrigation $\partial Y / \partial I$ may be determined as the slope of the function. (The differential is specified as being a partial derivative in recognition of other inputs such as sunshine hours, fertilizer applications, and others). Assuming that one has reliably determined the irrigation schedule that produces a yield-irrigation pair, determining the optimal schedule for another seasonal irrigation total that is a very small increment ΔI greater than (or less than) the known total is accomplished by finding the schedule that increases (or

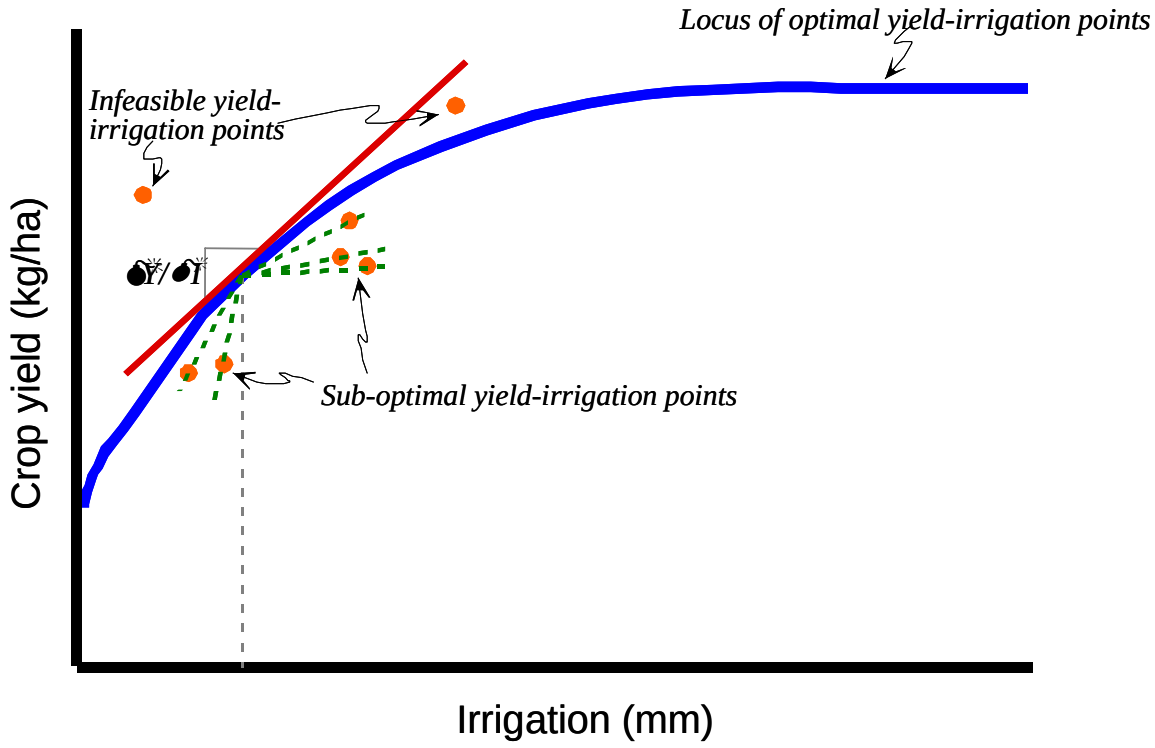

Figure 11. Optimal, Sub-Optimal, and Infeasible Transitions on the CWPF

decreases) crop yield by $\frac{\partial Y}{\partial I} \cdot \Delta I$. In the event that a sub-optimal change is made to the irrigation schedule, the new yield-irrigation point will be below the optimal crop-water production function. The transition pathway to the new point proceeds along a slope less than $\partial Y / \partial I$ in the case of adding irrigation and a slope greater than $\partial Y / \partial I$ in the case of subtracting irrigation.

This issue of optimal and sub-optimal transitions in yield-irrigation space is complicated somewhat by the fact that changes in total seasonal irrigation are accomplished by changes in the season-long irrigation schedule, which has components for multiple application periods. Thus, in order to determine the "true" value of $\partial Y / \partial I$ for the given point on the optimal crop-water production function, one must consider YIG values for all irrigation periods in the growing season. However, there are some important issues to be considered in computing and using YIG values.

First, the process of computing irrigation period-wise YIG values must be defined. For a given pre-existing irrigation schedule, it is a simple matter to add or subtract a small depth of irrigation in each irrigation period (independently of additions and subtractions in other periods); then for each period-wise change, the resultant change in crop yield can be divided by the irrigation change depth to produce a YIG value. Two important questions must be answered regarding this technique. What should be the depth of irrigation used for the incremental addition and subtraction in each period, and

should YIG values be defined based on irrigation additions, subtractions, or both? The results from repeated trials answer these two questions. An incremental depth of 10 mm adequately preserves the value of the differential $\partial Y / \partial I$ and also provides a large enough denominator in the ratio $\frac{\Delta Y}{\Delta I}$ to avoid numerical instability. When it is possible, the use of both additions and subtractions allows for calculation of a mean YIG value at the differential, but low pre-existing irrigation depths may make YIG calculation using incremental subtractions impossible (e.g., if pre-existing irrigation for a given period is 8 mm, it is not possible to subtract 10 mm). The final YIG calculation formula for each irrigation period *ip* is thus:

$$YIG_{ip} = \begin{cases} \dfrac{Y\left[I(I_{ip} + 10mm)\right] - Y\left[I(I_{ip} - 10mm)\right]}{20mm}, & if\ I_{ip} \geq 10mm \\ \dfrac{Y\left[I(I_{ip} + 10mm)\right] - Y\left[I(I_{ip} = 0)\right]}{\left(I_{ip} + 10mm\right)}, & if\ I_{ip} < 10mm \end{cases} \quad \textbf{(25)}$$

where the notation $Y\left[I(I_{ip} + 10mm)\right]$ signifies the crop yield produced with an irrigation schedule where irrigation in period *ip* is increased by 10 mm, $Y\left[I(I_{ip} = 0)\right]$ signifies the crop yield produced with an irrigation schedule where irrigation in period *ip* is 0 mm, etc.

A second major issue to consider in the calculation and utilization of YIG values is to appreciate the meaning of inter-period differences in YIG values. Figure 12 shows the complete season-long set of daily YIG values for the case of maize growth simulated for Eldoret, Kenya, short rains 1984, with the 400 mm total irrigation schedule shown (the schedule is for one day periods). It is obvious in this graph that YIG values vary greatly from –3 kg/ha/mm to almost 16 kg/ha/mm. (The negative values occur early in the season and are related to how early irrigation discourages enhanced root growth that may be important during drought in later stages.) Some of the differences in YIG values are easily explained. For example, there are noticeable "dips" in the series at days 129-134 and selected days between 182 and 194, and each of these periods has sustained irrigation. Another important trend is the two modes peaking at approximately days 92 and 178, respectively; these modes correspond to the important phenological stages of intensive leaf growth and ear formation, respectively. The importance of grain yield sensitivity to drought stress in these periods has been quantified by Doorenbos and Kassam (1979), among others. There are, however, some inter-period differences that require further interpretation. There exist strong differences in YIG values among irrigation periods for which there is irrigation scheduled. For example, day 103 (20 mm scheduled) has a YIG value of 14.3 kg/ha/mm, much greater than the value of 6.1 kg/ha/mm for day 129 (5 mm scheduled). These strong differences can also be found in comparing irrigated and non-irrigated periods: day 92 (zero irrigation scheduled) has a

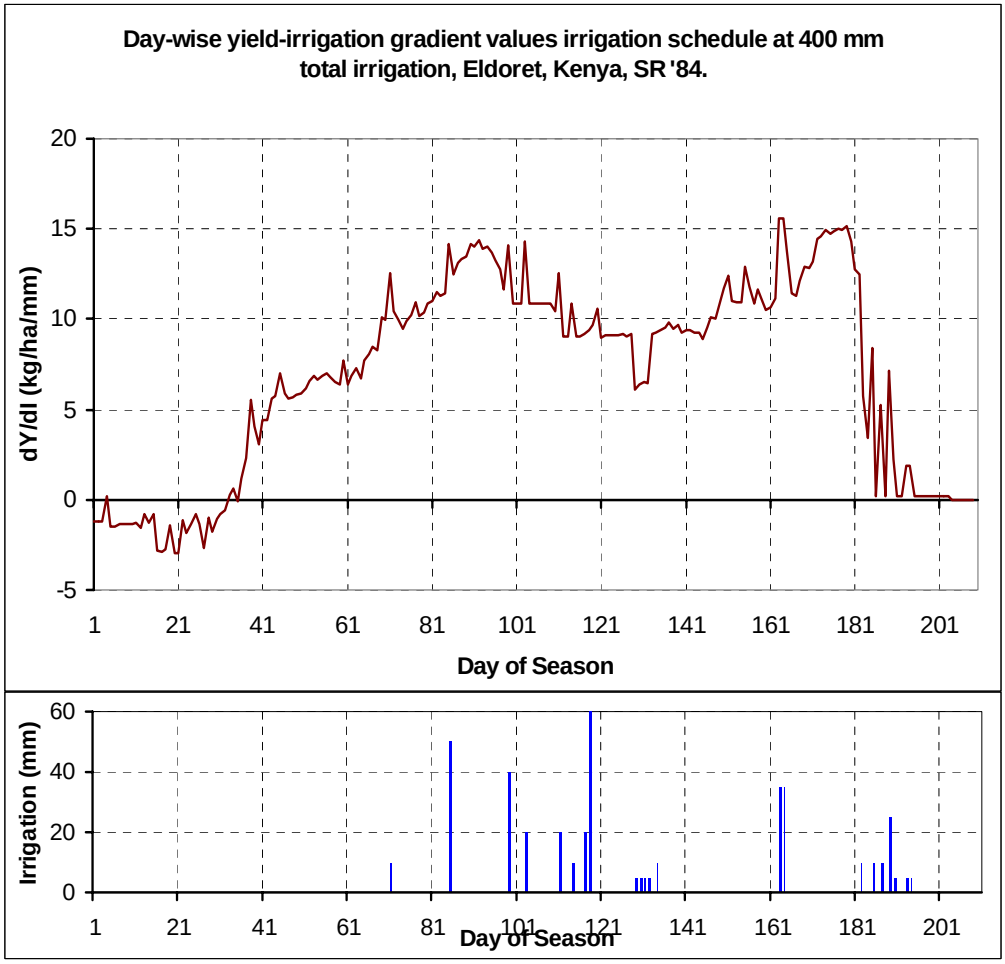

Figure 12. Yield-Irrigation Gradient (YIG) Values for a Case Study of Maize Grown under the Irrigation Schedule Shown

YIG value of 14.4 kg/ha/mm, which is greater than that for day 103 or day 129. These comparisons seem to suggest that one could take at least some of the 5 mm scheduled for day 129 and reallocate it to either day 103 or day 92 to achieve higher crop yield. Assuming that very small reallocations do not significantly alter YIG values, if 5 mm were transferred from day 129 to day 92, the crop yield would be expected to increase from 8474 kg/ha to 8515 kg/ha. This change in itself is small, but it might very well be possible to conduct several similar reallocations to improve crop yield substantially using the same total irrigation amount. Thus, it is seen that the original irrigation schedule is sub-optimal. If one were to start from this schedule in order to move to a different total irrigation amount, great care must be taken to insure that movement towards optimality takes place. Thus, another important conclusion to be drawn from this examination is that the starting point for deriving new, optimal irrigation schedules matters a great deal. Without significant a priori knowledge of an irrigation schedule's performance in a particular case, it is impossible to know whether or not it lies on the optimal crop-water production function. The situation shown in Figure 11 must now be understood as being

somewhat idealized. Indeed, the only point that a priori can be assumed to exist on the optimal crop-water production function is the zero irrigation point. Therefore, this point may well be the best choice for a starting point for irrigation optimization without additional knowledge.

A final issue to consider is how YIG values are to be best used in the irrigation planning process. As was discussed above in reference to Figure 12, for any irrigation schedule applied to a singular case, the set of irrigation period-wise YIG values may be computed and compared to each other. As has also been discussed, significant inequity of YIG values for irrigated periods may signal sub-optimality of the existing irrigation schedule, but due to phenological sensitivities, it is reasonable to assume that overall YIG differences will exist, even for optimal schedules. An irrigation planning algorithm can capitalize on these YIG differences. When it is desired to add irrigation to the seasonal total, it is readily apparent that the best period in which to apply it is the period having the maximum YIG value. Likewise, when it is desired to subtract irrigation from the seasonal total, it is most desirable to subtract it from the period having the minimum YIG value. The ability to apply this "Up-Max/Down-Min" (UMDM) rule is where lies the true utility of the YIG concept.

Three separate versions of the YIG technique have been developed and are described next: Simple YIG, Iterative YIG, and Randomized Iterative YIG. Schematics of the manner by which each algorithm functions are shown in Figure 13a-c.

4.2.1. Simple YIG (SYIG)

The "simple YIG" algorithm is a heuristic planning method that allocates water using one half of the aforementioned UMDM rule. Starting from the zero irrigation point – this is the only optimal point known a priori – YIG values are computed for all irrigation periods. Irrigation is then allocated to the period having the highest YIG value, and a new point on the crop-water production function is then estimated. Thus, the allocation rule is "Up-Max" only. The process is then repeated with the newly determined irrigation schedule taken as being fixed: a new set of YIG values is computed with the recently allocated irrigation increment in place, and so on. Figure 13a illustrates the concept of successive points on the CWPF being determined by "marching up" the curve. In implementation of this algorithm, there are at least three parameters that require consideration as to their effect on algorithm performance and computational efficiency: irrigation period length, irrigation increment, and allocation dispersion. Analysis of algorithm sensitivity to irrigation period length and irrigation increment finds that the derived CWPF's are somewhat sensitive to these parameter values in an inconsistent manner. The range of variation with changes in these two parameters is not overwhelming (within a few percent), but the inconsistency in response does suggest that the algorithm is not fully optimal.

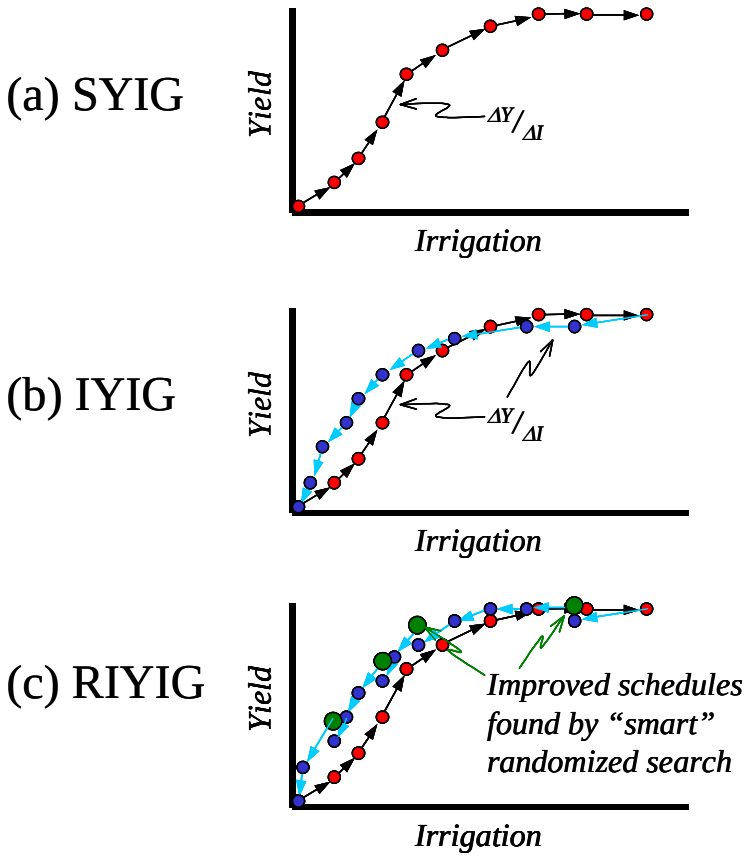

Figure 13. Schematics of CWPF Determination by 3 YIG Algorithms

Interest in the third parameter, allocation dispersion, is motivated by the observation in YIG time series (such as in Figure 12) that modes of high YIG values often are sustained over several irrigation periods. That observation begs the question of whether it is best to schedule irrigation application in the single period having the absolute highest YIG value or to disperse the incremental irrigation amount over several periods in the mode of YIG values. Testing of various allocation rules found that variation with dispersion was within a few percent. The best performing rule did practice some dispersion of irrigation allocation about the highest YIG value but required that all periods receiving irrigation be ranked contiguously at the top of the YIG value distribution.

Every time a set of YIG values is computed, the simple YIG algorithm requires two crop simulations for each irrigation period having non-zero pre-existing irrigation and one crop simulation for each irrigation period having no pre-existing irrigation. YIG values must be computed for each transition moving up the crop-water production function. These transitions start from zero irrigation, move by the chosen irrigation increment, and end at the full-yield irrigation when all YIG values are zero. Thus, the number of crop simulations $N_{CS,simpYIG}$ required by the simple YIG algorithm at a maximum is:

$$N_{CS,simpYIG} = \frac{I_{full-yield}}{\Delta I_{trans}} \cdot \left(2 \cdot N_{ip}\right) \quad \textbf{(26)}$$

where $I_{full\text{-}yield}$ is the irrigation amount at the full-yield plateau, and ΔI_{trans} is the irrigation increment for each transition up the crop-water production function.

In the Nile DST Agricultural Planning Module, ΔI_{trans} is 10 mm for all crops except cassava, which has ΔI_{trans} of 30 mm. The reason for the difference is cassava's longer growing season; computer run time is brought down to reasonable levels by the higher ΔI_{trans}. Irrigation period length is 10 days for all crops. Examples of computer run times are given in Section 5. For each 10 mm increment, the increment can be split up and dispersed to as many as 5 irrigation periods, although typically the increment is concentrated in 1 or 2 periods.

4.2.2. Iterative YIG (IYIG)

The "iterative yield-irrigation gradient" (IYIG) irrigation planning algorithm is conceptually distinct from the simple YIG method in that it fully utilizes the "up-max/down-min" (UMDM) rule that was suggested above. That is, differential irrigation allocations are made as both additions and subtractions, with additions going to periods having maximum YIG values, and subtractions coming from minimum YIG periods. The simple YIG algorithm performs only the irrigation additions. The algorithm proceeds first monotonically upward (irrigation additions) in yield-irrigation space until a yield-irrigation point having all zero YIG values is reached. Then, the algorithm proceeds monotonically downward (irrigation subtractions) to the zero irrigation point. This up-down movement is the source of the "iterative" name. Figure 13b shows schematically the "up and down" path.

In implementation it is found in many cases that yield-irrigation response is quite different in the downward pass from that of the upward pass. Graphed in the yield-irrigation domain, the downward pass CWPF is generally improved over the upward pass CWPF, although a "figure-8" loop is sometimes formed with a small decrease in performance at the highest irrigation values for the downward pass. The change in performance is accompanied of course by changed irrigation schedules between the two passes for any given seasonal total. Improvements in the CWPF are especially striking at the lowest seasonal irrigation totals for some cases. This hysteretic behavior is driven by the fact that YIG values at each yield-irrigation point are influenced by the totality of the pre-existing irrigation schedule at that point, which may include irrigation applications not extant when water was originally allocated to each period. As the changes from the "down-min" process accumulate, CWPF performance improves.

These improved results do of course come at greater computational cost. The number of crop simulations required by the IYIG algorithm is equal to the sum of the upward and downward passes. The upward pass is simply the same as the simple YIG

procedure discussed above. The downward pass requires fewer crop simulations since YIG values need be computed only for periods having non-zero irrigation allocations at each yield-irrigation point. A crude means to approximate the number of non-zero irrigation periods in the downward pass is to assume that this number varies linearly from N_{ip} at the full-irrigation point to zero at the zero-irrigation point. Using this approximation the total number of crop simulations for both the upward and downward passes $N_{CS,IYIG}$ is:

$$N_{CS,IYIG} = \frac{I_{full-yield}}{\Delta I_{trans}} \cdot \left(2 \cdot N_{ip}\right) + \frac{1}{2} \cdot \left[\frac{I_{full-yield}}{\Delta I_{trans}} \cdot \left(2 \cdot N_{ip}\right) \right] = \frac{3 \cdot I_{full-yield} \cdot N_{ip}}{\Delta I_{trans}} \qquad \textbf{(27)}$$

which is most likely biased towards over-estimation for reasons mentioned above.

Tests of IYIG algorithm sensitivity to irrigation increment amount ΔI_{trans} show that very small increments (e.g., 1 mm) can result in improved results over more moderate increments (e.g., 10 mm); comparison of the irrigation schedules produced under these increments at common seasonal irrigation totals also show appreciable differences in their temporal distribution of irrigation applications. Thus the choice of the irrigation allocation increment influences the character of irrigation schedules produced by the IYIG algorithm. This observation raises the question of whether the IYIG algorithm can be improved to dissociate the seasonal character of the irrigation schedules produced from the parameterization used. As the algorithm proceeds in its downward pass, it is desirable for it to know when it has "gotten off-track" and produced irrigation schedules detrimental to the performance of schedules to be derived at lower seasonal irrigation totals. This concern motivates the form of the final YIG algorithm presented next.

As implemented in the Nile DST, the IYIG algorithm has the same values of ΔI_{trans}, irrigation period length, and number of periods that may receive irrigation allocations as for the Simple YIG algorithm. When hysteresis loops are formed between the upward and downward passes, the software sorts through both passes to construct a composite function equal to the higher of the two passes at all points.

4.2.3. Randomized Iterative YIG (RIYIG)

The "randomized iterative yield-irrigation gradient" (RIYIG) algorithm operates in a manner similar to that of the IYIG algorithm but with an additional computational component that emulates a characteristic of self-awareness. The observation was made in the previous section that the IYIG algorithm can underestimate the optimal yield-irrigation curve as it transitions repeatedly to new yield-irrigation points. This phenomenon reveals the value of a means by which to test any yield-irrigation point to determine whether or not it truly is optimal. That is, a reliable method is needed to determine if there exists any irrigation schedule that produces higher crop yield than the irrigation schedule in question for the same seasonal irrigation total. (Conversely, a test could determine if the same yield could be produced with an irrigation schedule having a

lower seasonal irrigation total, but this is more difficult to accomplish). The RIYIG algorithm includes just such an optimality test based upon repeated application of randomized irrigation schedules.

The method of randomized schedule testing presented here is inspired by Monte Carlo simulation, which is typically used to derive the statistical properties of model output when the statistical properties of the model input are known. The feature of the Monte Carlo technique that is most attractive to the application of optimality testing is the use of repeated simulations based upon randomized inputs. The "randomized irrigation schedule test-1" (RIST-1) used here is a modification of Monte Carlo analysis as follows. For a given total seasonal irrigation amount, a large number of randomized irrigation schedules are produced such that each schedule's total allocation is the amount of interest. The crop model is then run for each irrigation schedule, the crop yield produced under that schedule is computed, and the yield is saved. After all the irrigation schedules have been simulated, the highest crop yield value obtained is compared to the yield-irrigation point that is being tested. If the tested point's crop yield is lower than the maximum produced by the randomized schedules, the tested yield-irrigation point is determined to be sub-optimal, and a better schedule has been produced by the randomization process. Experience with different randomization schemes has shown that in order to find an irrigation schedule producing greater crop yield than a schedule produced by the IYIG algorithm, the randomization process must use the original IYIG schedule as a base and proceed with some amount of controls. In only a handful out of tens of thousands of tests did irrigation schedules produced from completely blind randomization achieve greater crop yields than IYIG schedules of the same seasonal total irrigation. The more sophisticated approach based upon IYIG schedules found improved schedules in almost all cases where at least 1000 randomizations were tested.

The RIYIG algorithm utilizes the RIST-1 test for optimality at periodic "evaluation points" in the downward pass through the yield-irrigation domain. At each evaluation point a large number of randomized schedules are produced based upon the schedule found by the IYIG downward pass at that point so that all schedules have the same seasonal irrigation total. If a schedule producing greater crop yield than the base schedule is found, the randomized schedule becomes the new base and the process continues. Thus the completed downward pass possibly includes several jumps where improved schedules were found at the evaluation points. These jumps can be smoothed by short simple YIG implementations beginning at the top of each jump and moving upward until intersection with the rest of the CWPF. In implementation, 9 evaluation points have been used for the present case studies (at 90%, 80%, …, and 10% of the gains from irrigation), and 1000 randomized schedules were used in the RIST-1 procedure at each evaluation point. The RIYIG algorithm consistently produced improved results in CWPF's over the IYIG method.

The computational requirements of the RIYIG algorithm are easily found by adding the number of randomized schedule simulations and smoothing simulations to the number of simulations used in the IYIG algorithm. The randomization process itself is also added to the actual computations performed, but this process is trivial compared to

the crop simulation accompanying each iteration. Each evaluation point requires a smoothing step, and each smoothing step has been observed to require on average three to six simulations. In general, the number of crop simulations required by the RIYIG is:

$$N_{CS,RIYIG} = \frac{I_{full-yield}}{\Delta I_{trans,up}} \cdot \left(2 \cdot N_{ip}\right) + \frac{1}{2} \cdot \left[\frac{I_{full-yield}}{\Delta I_{trans,down}} \cdot \left(2 \cdot N_{ip}\right)\right] + N_{rs} \cdot \left(N_{sim} + N_{smooth}\right) \quad \textbf{(28)}$$

where N_{rs} is the number of evaluation points to be performed, N_{sim} is the number of randomized schedule simulations performed at each point, and N_{smooth} is the number of smoothing simulations at each evaluation point.

In the Nile DST, the RIYIG algorithm is implemented with the following parameters for non-cassava crops: ΔI_{trans} is 10 mm, irrigation period length is 10 days, 11 randomization steps ("breakpoints") are used on the downward pass, and each breakpoint includes evaluation of 500 randomized irrigation schedules. For cassava, ΔI_{trans} is 30 mm, irrigation period length is 10 days, 8 breakpoints are used, and each breakpoint includes 200 randomized irrigation schedules.

5. Case Studies

5.1. Sensitivity of CWPF's to Weather, Planting Date, and Algorithm Choice

The first case study will look at assessment of maize cultivated at Eldoret, Kenya, and the changes in the crop-water production function resulting from different choices of planting date (with accompanying different weather) and choice of CWPF algorithm. Figure 14 shows a CWPF output graph from the Nile DST for this case. Each curve is shown in a different color and corresponds to a different set of parameters. Table 1 below lists these parameters. Meteorological data from the year 1984 was used for all simulations.

Table 1. Parameters for CWPF's in Figure 14 (maize at Eldoret, Kenya, 1984 meteorology).

Curve Color	"Planting Location"	Planting Date	Algorithm
Red	1	March 15	MST
Blue	2	March 15	SYIG
Gray	3	March 15	IYIG
Green	4	March 15	RIYIG
Pink	5	October 1	MST
Light Blue	6	October 1	SYIG
Black	7	October 1	IYIG
Gold	8	October 1	RIYIG

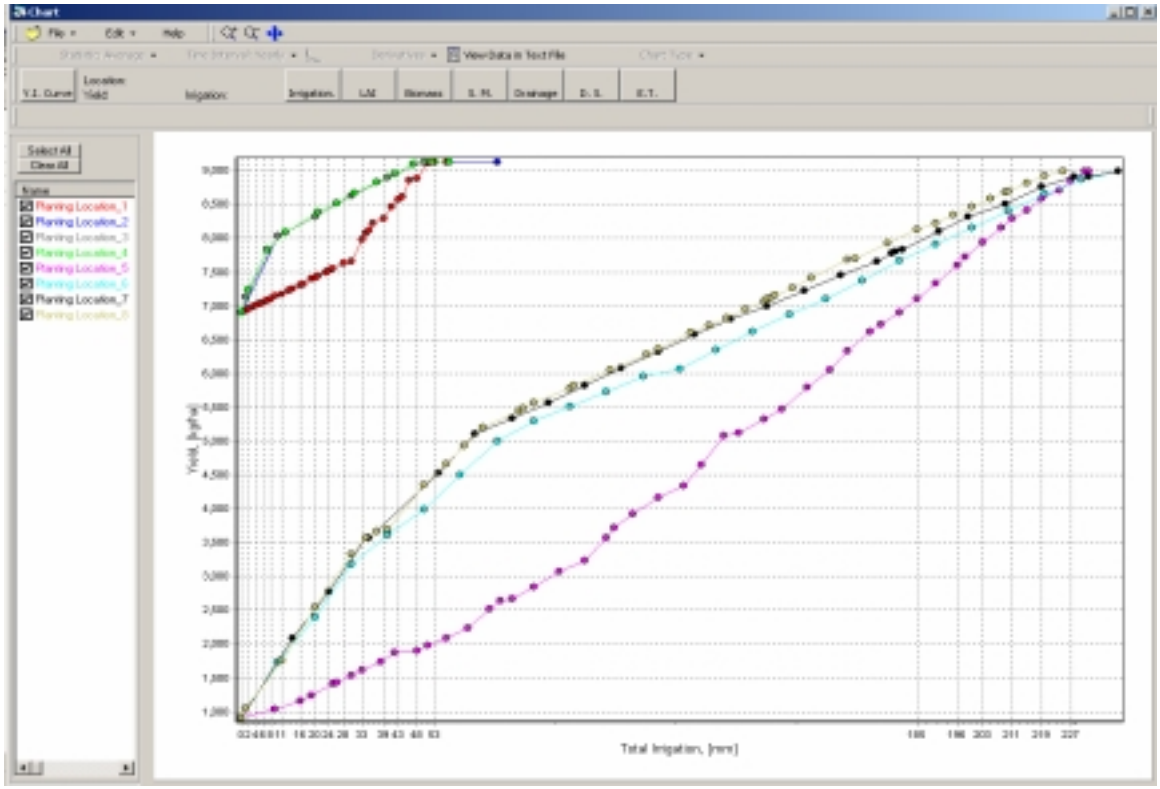

Figure 14. CWPF's for Maize Grown at Eldoret, Kenya

The most obvious difference among results in that between planting dates. The results for the March 15 planting date have rainfed yield of slightly less than 7000 kg/ha. Rainfed yield for the October 1 planting date is just less than 1000 kg/ha. This difference is caused by the differences in rainfall after each planting date, the March planting being followed by more precipitation than that in October. Consequently, the irrigation necessary to reach maximum possible crop yield is much different: about 50 mm for the March planting, and about 225 mm for the October planting. In this case, the fully irrigated yields are quite similar but not exactly equal: about 9150 kg/ha for the March planting, and about 9000 kg/ha for the October planting. It is expected that fully irrigated yields will change from season to season and year to year. Maximum yield levels are determined by non-moisture factors such as temperature and incoming sunlight, which change each year resulting in variable maximum yield. This point will be even more apparent in section 5.2 below.

Just as rainfed yield increased in this example, it is possible for growing season rainfall to be wholly adequate for plant needs. In that case, the CWPF will be shown in the Nile DST as a single point on the vertical axis. This should be interpreted as a horizontal line extending to the right from that point. Irrigation will not increase crop yield in that case. Similarly, attention should be paid to the numerical scale of the vertical axis. Figure 15 shows a CWPF for cassava grown at Entebbe, Uganda, (planting date March 15, meteorological year 1984). Although the CWPF appears to have

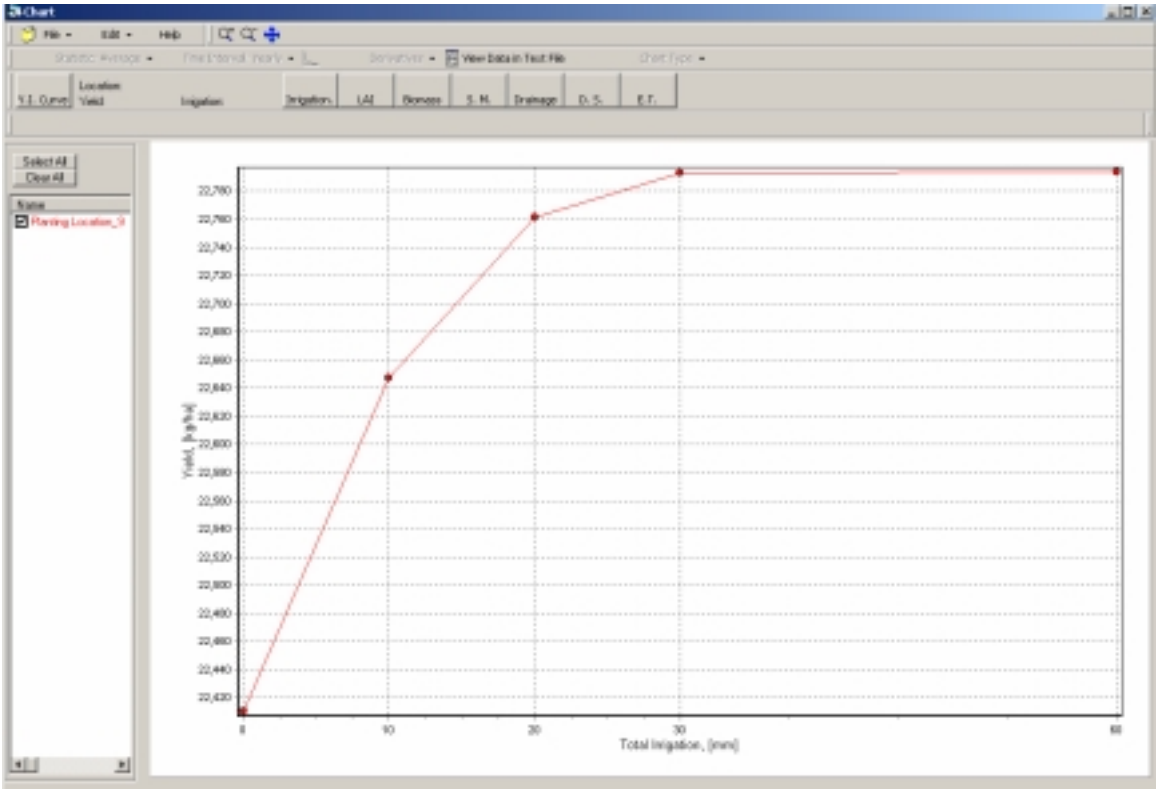

Figure 15. CWPF for a Case of Cassava Grown at Entebbe, Uganda

pronounced curvature, observing the difference between rainfed and fully irrigated yields reveals little difference between the two levels; the curve is virtually flat.

Comparison of CWPF's from the different algorithms also yields important insights. The MST-determined CWPF's (shown in red for March planting and pink for October planting, respectively) are readily seen as sub-optimal compared to the YIG functions. The rainfed and fully irrigated points are common across algorithms, but the MST functions produce less crop yield in the deficit irrigation region. The primary reason for the difference is that the MST algorithm does not differentiate the relative importance of drought stress among different portions of the growing season. As can be seen in the yield reduction coefficients of Doorenbos and Kassam (1979), discussed in section 2.1 above, crop yield suffers from drought stress in some growth stages (such as flowering) more so than in others. Nevertheless, the MST method does reproduce a likely tendency of an irrigator to irrigate whenever the plant appears stressed with differing tolerances for that stress.

The CWPF's determined by the three YIG algorithms have some apparent differences for the October planting date but appear almost identical for the March planting date. Both cases are common. In general, for locations having smaller differences between rainfed and fully irrigated yield CWPF's determined by the three YIG methods will be similar. However, when rainfed yields are very low, the three

methods tend to produce different results. The RIYIG algorithm is self-verifying in its use of randomized checks and can therefore be counted on to provide optimal CWPF's in all cases. The IYIG and SYIG algorithms are progressively less reliable in achieving the best possible CWPF's, but their computational requirements and computer run times are much lower. Figure 16 shows the computer run times for the 8 CWPF's shown in Figure 14. The runs were performed on a 1.06 GHz Pentium II PC. The SYIG method is obviously the fastest, but at times gives CWPF's that may drop below optimal yield levels by a few percent. The Nile DST user is counseled to consider the tradeoff existing between execution time and guaranteed optimality of results. It is likely that SYIG or IYIG is an appropriate choice for initial assessments for large numbers of planting locations and conditions, and RIYIG is appropriate for more detailed "fine-tuning" types of assessments.

The differences in crop yield produced by each of the planning algorithms for the same amounts of seasonal irrigation are due to differences in scheduling of irrigation by the methods. Figure 17 shows the MST irrigation schedule for the October 1 planting date for 175 mm total seasonal irrigation. The RIYIG produced schedule for the same planting date and 174 mm irrigation is shown in Figure 18. The differences in the schedules are easy to find. The MST schedule has fairly equal applications of roughly 28 mm for a period of several ten-day periods in a row. The RIYIG schedule is much more targeted with large applications above 50 mm in critical growth stages. As was discussed in Section 4, the MST methods lack of differentiation among growth stages has led in this case to irrigation to equalize drought stress across growth phases. Improved results consistent with phenological needs are identified by the RIYIG method's explicit optimization emphasis.

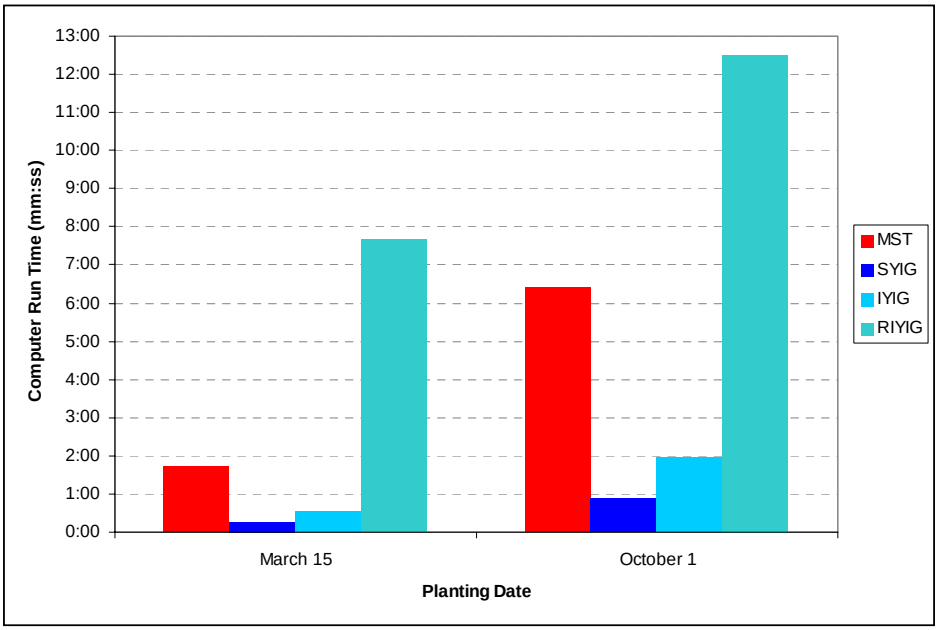

Figure 16. Computer Run Times to Determine CWPF's Shown in Figure 14

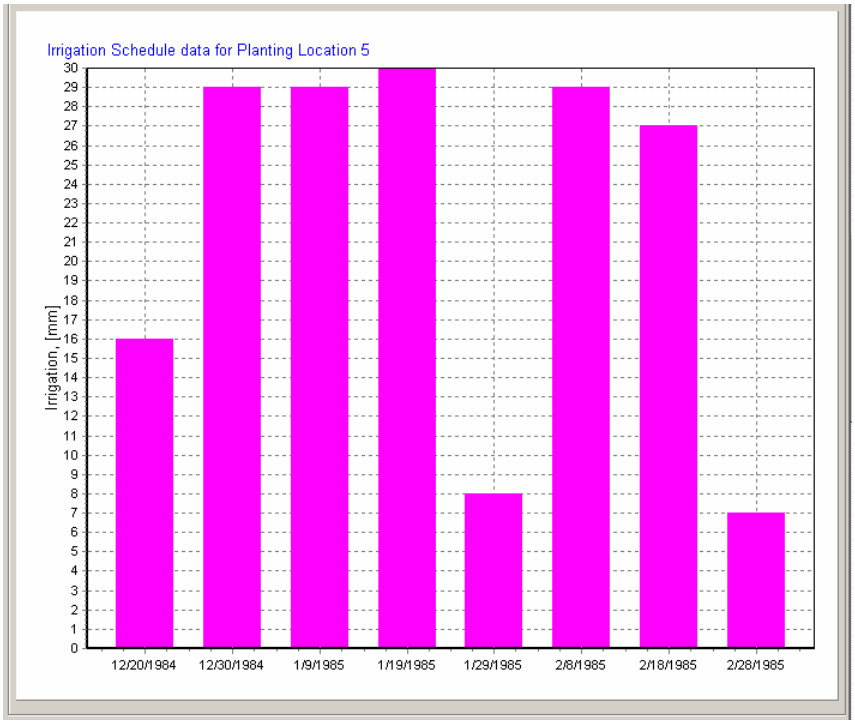

Figure 17. MST Irrigation Schedule for 175 mm Seasonal Irrigation

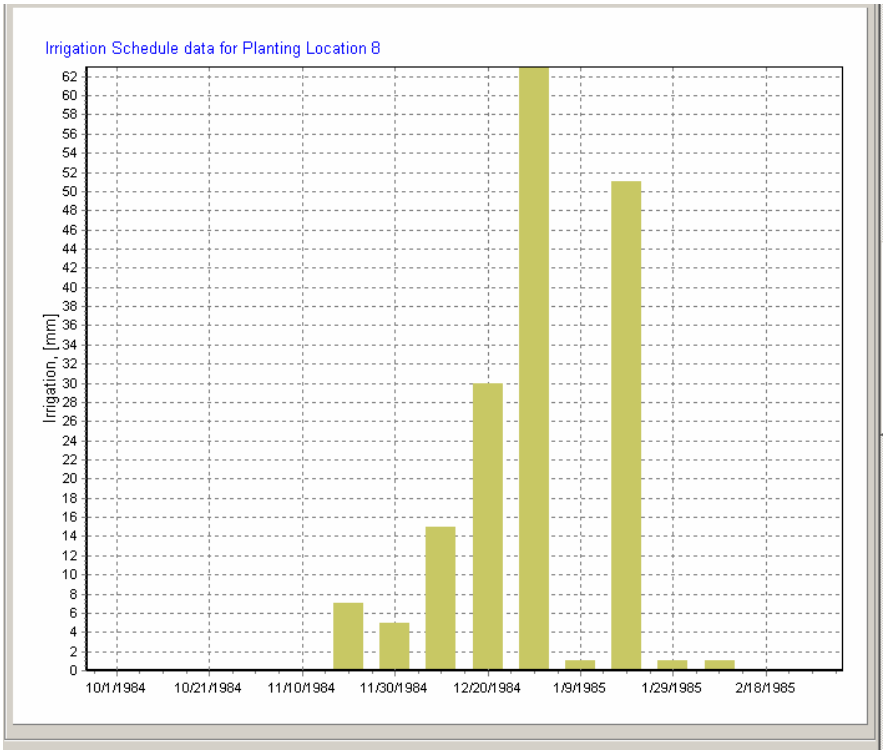

Figure 18. RIYIG Irrigation Schedule for 174 mm Seasonal Irrigation

5.2. Assessing Agricultural Response to Climate Variability

An important analysis that can be performed using the Nile DST Agricultural Planning module is to assess the variability of yield-irrigation response with climate variability. By determining CWPF's at a single location with constant management parameters for all meteorological years available in the database, a probabilistic understanding of crop yield and irrigation needs can be found.

Figure 19 presents CWPF's for maize grown at Biharamulo, Tanzania, with a planting date of March 15 for 17 different years of meteorological conditions. There is significant variability evident at this location. Rainfed yield has a maximum of about 8700 kg/ha and a minimum of about 2200 kg/ha. The maximum yield actually occurs in 2 years from the record, and both of these values represent circumstance where no additional irrigation is needed by the crop (indicated by single points on the graph). The median rainfed yield is just over 5800 kg/ha, and the central 50% of rainfed yield values (between the 25^{th} and 75^{th} percentiles) vary from 4700 kg/ha to 6000 kg/ha. Thus, while overall variability is quite high, there is a strong central tendency present where half of all years have rainfed yield within a more narrow range.

Fifteen of the 17 meteorological years have possible significant gains in crop yield from irrigation. Crop yield increases range from 33% to 390% over rainfed values. However, the irrigation necessary to achieve these gains also has significant variability – from about 80 mm to 180 mm. The slopes of each of these 15 CWPF's are remarkably similar, which is not always the case.

All of these forms of variability are caused by climatic factors; rain, temperature, and available sunlight are the principal determinants. Use of the stochastic crop-water relationship shown here can be very useful for questions of risk and reliability. For example, if an irrigation manager knew that it would be possible to supply 80 mm of irrigation to this site, he or she might want to know the expected crop yields resulting from that irrigation. By looking at the distribution of CWPF points at 80 mm irrigation, the manager could see that:

- Minimum crop yield would be 6000 kg/ha;
- Maximum crop yield would be 8700 kg/ha;
- Median crop yield would be about 8100 kg/ha;
- In the middle half of all years, crop yield would range between 7550 and 8400 kg/ha.

Climate variability may also be correlated with events known to influence patterns of rainfall and temperature. There have been significant findings of climate correlations in the Nile Basin with El Nino and La Nina phenomena (e.g., Indeje et al. 2000, Nicholson and Selato 2000, Mutai et al. 1998, etc.). Table 2 shows the results of simulating rainfed maize yields at Bungoma, Kenya, for planting October 1, using 9 years of meteorological data. The "El Nino Southern Oscillation" ENSO condition is also shown in this table. There is a clear correlation of higher rainfed crop yields in years

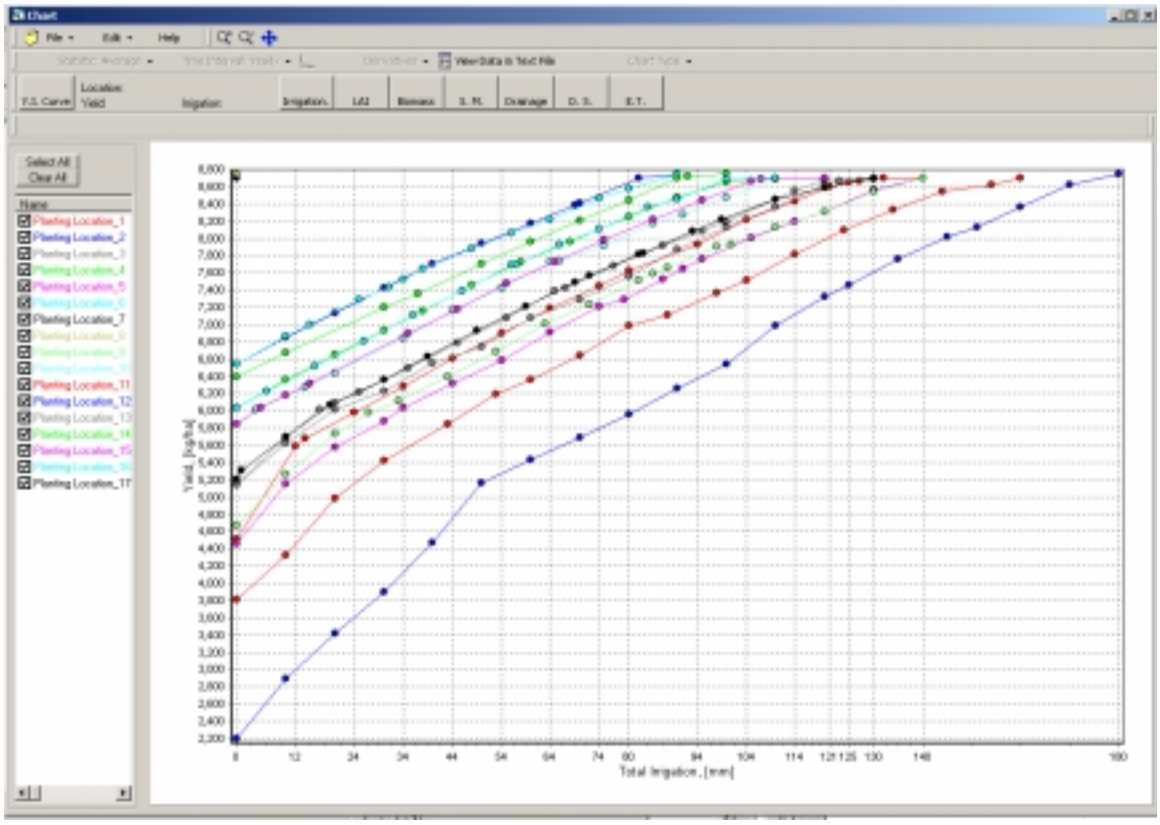

Figure 19. Variability of Yield-Irrigation Response with Climate

Table 2. Ranking of rainfed maize yields (October 1 planting) at Bungoma, Kenya, for 9 meteorological years.

Rank	Year	Rainfed Yield (kg/ha)	ENSO Condition*
1	1984	7,085	EN + 1
2	1972	6,705	EN
3	1985	6,621	--
4	1973	5,966	EN + 1
5	1983	5,798	EN
6	1976	5,126	LN
7	1974	5,076	LN
8	1975	4,546	LN
9	1971	2,676	LN + 1

*ENSO condition abbreviations: EN – same year as El Nino occurrence, EN + 1 – one year after El Nino, LN – same year as La Nina occurrence, LN + 1 – one year after La Nina (1985 fits none of these conditions)

during and immediately after El Nino events. There is similarly a clear decrease in rainfed yields correlated with La Nina events and their immediate aftermath. Similar analysis for fully irrigated yields shows no correlation since irrigation serves to compensate for the dry conditions associated with ENSO events. Thus, phenomena such as ENSO events can be an important tool for predicting rainfed yield and irrigation needs, but not ultimate crop yields.

5.3. Irrigation Management

Allocation of limited irrigation water to multiple crops in a multi-season rotation or for simultaneous plots is an important management task. Use of the information given by CWPF's can assist the farmer or irrigation manager in this difficult task. Figure 20 shows CWPF's for 3 crops planted simultaneously. The simulations used a planting date of March 15, at Biharamulo, Tanzania, and meteorological year 1976. Maize is shown in red, wheat in blue, and dry bean in gray. The wheat CWPF is a single point indicating that the yield plateau exists under rainfed conditions. Therefore, for this case (subject to cultivar chosen and other management parameters) irrigation will produce no crop yield benefits. Rainfed yields for maize and dry beans are at moderate levels (different crops will have different relative magnitudes of crop yield as well as nutritional density). However, significant increases in yield are possible for both crop under irrigation. The water needed for full yield for maize is somewhat higher than for dry beans, roughly 90 mm for maize and 50 mm for dry beans. Under limited water availability there may not be enough for both fields to reach maximum yield. Moreover, the timing of water availability may also be a significant constraint.

Figures 21 a-b and 22 a-b show irrigation schedules for different yield-irrigation points for maize and dry bean in this case. In Figure 21a, a moderate seasonal total of 38 mm irrigation is concentrated mostly in one application on April 20 with a few very small applications in June and July; this would produce a yield of 7646 kg/ha. To achieve maximum yield of 8744 kg/ha using 90 mm of seasonal irrigation, applications are required from mid-April until August (Figure 21b). Moderate irrigation of 27 mm applied to dry beans would be concentrated in a single application in early June producing 2622 kg/ha (Figure 22a). Maximum dry bean yield of 3069 kg/ha would require 70 mm of irrigation applied from mid-April through late June. Thus, at moderate irrigation amounts the timing of irrigation needs for the crops is different. Even if water availability is constrained in time, it may be possible to supply water to both crops to achieve yield increases. The decision on water allocations would also take into account current prices, local demand, non-water production issues such as fertilizer needs, labor, and other important issues.

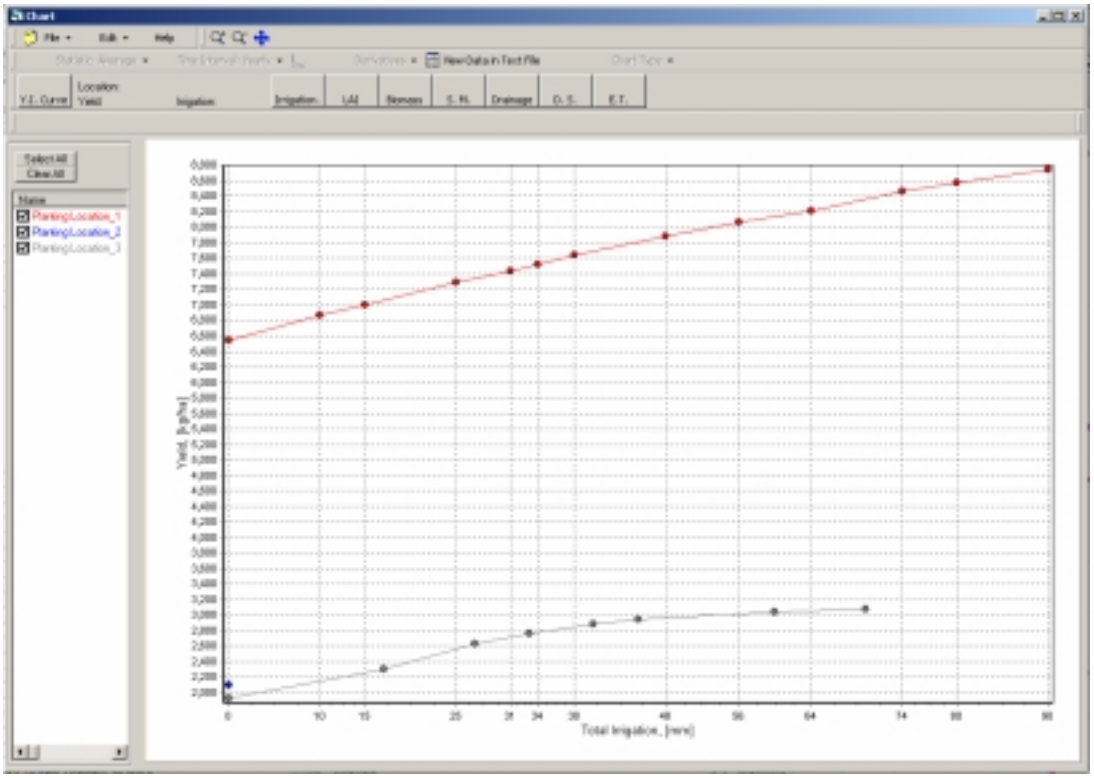

Figure 20. CWPF's for 3 Simultaneous Crops

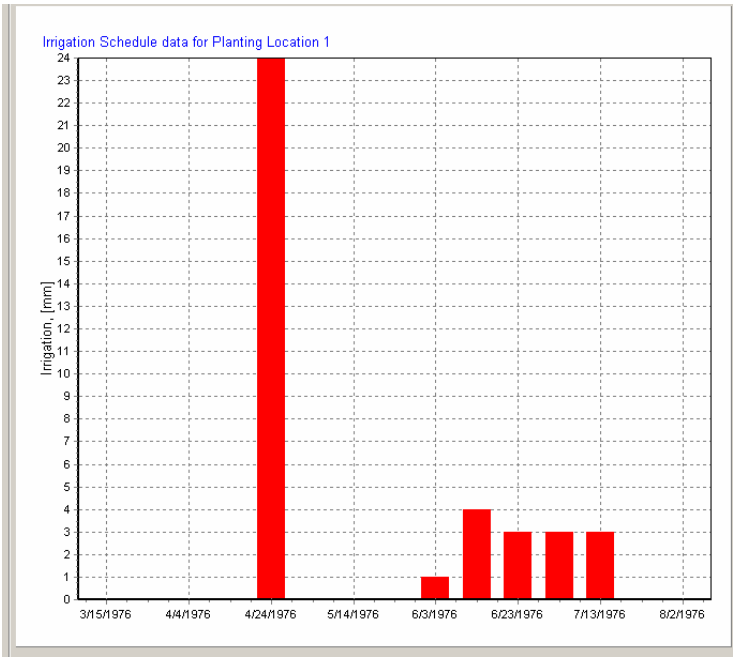

Figure 21a. Irrigation Schedule for Maize, Seasonal Total 38 mm

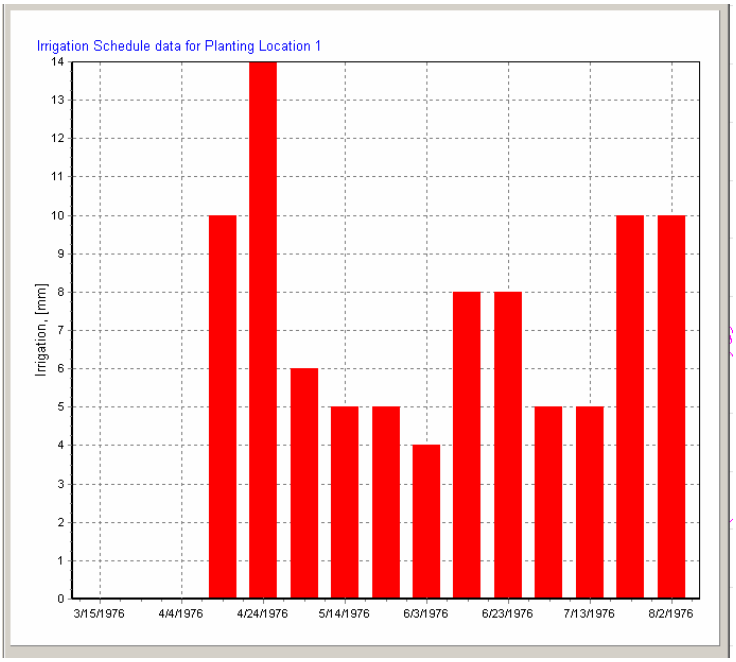

Figure 21b. Irrigation Schedule for Maize, Seasonal Total 90 mm

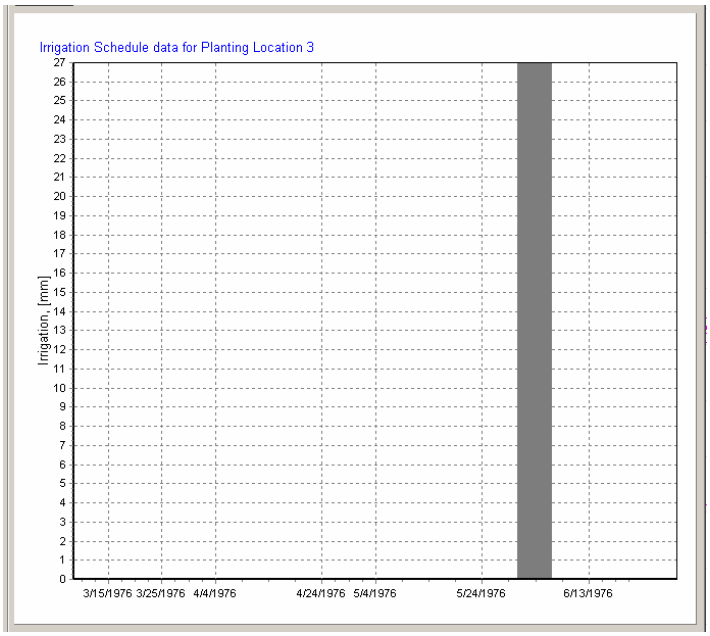

Figure 22a. Irrigation Schedule for Dry Bean, Seasonal Total 27 mm

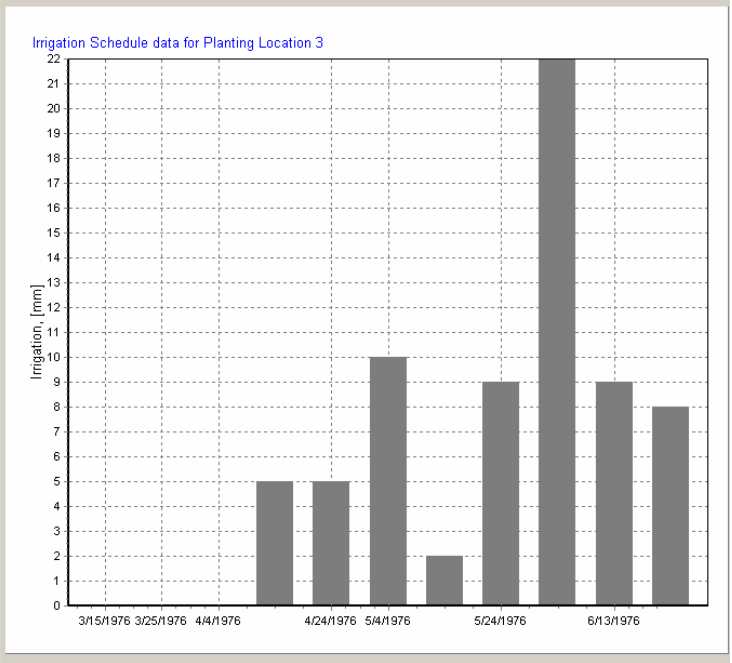

Figure 22b. Irrigation Schedule for Dry Bean, Seasonal Total 70 mm

6. Conclusion

The Nile DST Agricultural Planning module integrates several important technologies in order to provide useful information for planning and decision making relevant to agriculture and irrigation. Crop models, optimization techniques, databases, geographic information systems, and visualization tools are all included in a seamless fashion. This report has presented some of the types of analyses that may be conducted using the module, but this presentation is by no means exhaustive. By understanding the capabilities and underlying theory of the module's components described here, the user will be able to formulate and conduct useful assessments.

References

Alagarswamy, G., P. Singh, G. Hoogenboom, S.P. Wani, P.Pathak, and S.M. Virmani. 2000. "Evaluation and Application of the CROPGRO-Soybean Simulation Model in a Vertic Inceptisol." *Agricultural Systems.* Vol. **63**. pp. 19-32.

Allen, R.G., L.S. Pereira, D. Raes, and M. Smith. 1998. "Crop evapotranspiration - Guidelines for computing crop water requirements." FAO Irrigation and Drainage Paper no. 56. FAO, Rome, Italy.

Allen, R.G. and W.O. Pruitt. 1986. "Rational Use of the FAO Blaney-Criddle Formula." *Journal of the Irrigation and Drainage Engineering Division*. Vol. **112**(IR2). pp. 139-155.

American Society of Civil Engineers (ASCE). 1990. *Evapotranspiration and Irrigation Water Requirements*. Manuals and Reports on Engineering Practice no. 70. ed. M.E. Jensen, R.D. Burman, and R.G. Allen. ASCE, New York.

Blaney, H.F. and W.D. Criddle. 1950. "Determining Water Requirements in Irrigated Areas from Climatological and Irrigation Data." USDA Soil Conservation Service Technical Paper 96.

Brumbelow, K., and A. Georgakakos. 2001. "An Assessment of Irrigation Needs and Crop Yield for the United States under Potential Climate Changes." *Journal of Geophysical Research, Atmospheres.* Vol. 106(D21). 27,383-27,406.

Caravallo, H.O., E.A. Holzapfel, M.A. Lopez, and M.A. Marino. 1998. "Irrigated Cropping Optimization." *Journal of Irrigation and Drainage Engineering.* Vol. **124**(2). pp. 67-72.

Clarke, D. 1998. "CropWat for Windows: User Guide." FAO, Rome, Italy.

Dinar, A., K.C. Knapp, and J.D. Rhoades. 1986. "Production Function for Cotton with Dated Irrigation Quantities and Qualities." *Water Resources Research*. Vol. **22**(11). pp. 1519-1525.

Doorenbos, J. and A.M. Kassam. 1979. "Yield Response to Water." FAO Irrigation and Drainage Paper no. 33. FAO, Rome, Italy.

Doorenbos, J. and W.O. Pruitt. 1977. "Guidelines for Predicting Crop Water Requirements." FAO Irrigation and Drainage Paper no. 24 (2nd ed.). FAO, Rome, Italy.

English, M., and B. Nakamura. 1989. "Effects of Deficit Irrigation and Irrigation Frequency on Wheat Yields." *Journal of Irrigation and Drainage Engineering.* Vol. **115**(2). pp. 172-184.

Gabrielle, B., S. Menasseri, and S. Houot. 1995. "Analysis and Field Evaluation of the CERES Models Water Balance Component." *Soil Science Society of America Journal,* Vol. **59**. pp. 1403-1412.

Garrison, M.V., W.D. Batchelor, R.S. Kanwar, and J.T. Ritchie. 1999. "Evaluation of the CERES-Maize Water and Nitrogen Balances under Tile-Drained Conditions." *Agricultural Systems.* Vol. **62**. pp. 189-200.

Griffin, T.S., B.S. Johnson, and J.T. Ritchie. 1993. "A Simulation Model for Potato Growth and Development: SUBSTOR-Potato Version 2.0." IBSNAT Research Report Series 02. University of Hawaii, Honolulu.

Hexem, R.W. and E.O. Heady. 1978. *Water Production Functions for Irrigated Agriculture.* Iowa State Univ. Press, Ames, Iowa.

Holzapfel, E.A., M.A. Marino, A. Valenzuela. 1990. "Drip Irrigation Nonlinear Optimization Model." *Journal of Irrigation and Drainage Engineering.* Vol. **116**(4). pp. 479-496.

Jones, C.A. and J.R. Kiniry. 1986. *CERES-Maize: A Simulation Model of Maize Growth and Development*. Texas A&M University Press, College Station, Texas.

Linsley, R.K., M.A. Kohler, and J.L.H Paulhus. 1982. *Hydrology for Engineers*. 3rd ed. McGraw-Hill, New York

Martin, D.L., J.R. Gilley, and R.J. Supalla. 1989. "Evaluation of Irrigation Planning Decisions." *Journal of Irrigation and Drainage Engineering.* Vol. **115**(1). pp. 58-77.

Martin, D.L., J.R. Gilley, and R.W. Skaggs. 1991. "Soil Water Balance and Management." *Managing Nitrogen for Groundwater Quality and Farm Profitability.* ed. R.F. Follett, D.R. Keeney, and R.M. Cruse. Soil Science Society of America, Madison, Wisconsin.

Matthews, R.B. and L.A. Hunt. 1994. "GUMCAS: A model describing the growth of cassava (Manihot esculenta L. Crantz)." *Field Crops Research.* Vol. **36**. pp. 69-84.

Monteith, J.L. 1965. "Evaporation and Environment." *The State and Movement of Water in Living Organisms, XIXth Symposium*. Society for Experimental Biology. Cambridge University Press, Swansea, England.

Mugabe, F.T., and E.Z. Nyakatawa. 2000. "Effect of Deficit Irrigation on Wheat and Opportunities of Growing Wheat on Residual Soil Moisture in Southeast Zimbabwe." *Agricultural Water Management.* Vol. **46**. pp. 111-119.

Paul, S., S.N. Panda, and D.N. Kumar. 2000. "Optimal Irrigation Allocation: A Multilevel Approach." *Journal of Irrigation and Drainage Engineering.* Vol. **126**(3). pp. 149-156.

Penman, H.L. 1948. "Natural Evaporation from Open Water, Bare Soil, and Grass." *Proceedings of the Royal Society of London*. Series A, Vol. **193**. pp. 120-145.

Priestly, C.H.B. and R.J. Taylor. 1972. "On the Assessment of Surface Heat Flux and Evaporation Using Large-Scale Parameters." *Monthly Weather Review*. Vol. **100**(2). pp. 81-92.

Ritchie, J.T. 1972. "Model for Predicting Evaporation from a Row Crop with Incomplete Cover." *Water Resources Research*. Vol. **8**(5). pp. 1204-1213.

Ritchie, J.T. 1998. "Soil Water Balance and Plant Water Stress." *Understanding Options for Agricultural Production.* ed. G.Y. Tsuji et al. Kluwer Academic Publishers, Dordrecht, Netherlands.

Roman-Paoli, E., S.M. Welch, and R.L. Vanderlip. 2000. "Comparing Genetic Coefficient Estimation Methods Using the CERES-Maize Model." *Agricultural Systems.* Vol. **65**. pp. 29-41.

Smith, M. 1992. "CROPWAT: A Computer Program for Irrigation Planning and Management." FAO Irrigation and Drainage Paper no. 46. FAO, Rome, Italy.

Steele, D.D., E.C. Stegman, and B.L. Gregor. 1994. "Field Comparison of Irrigation Scheduling Methods for Corn." *Transactions of the American Society of Agricultural Engineers.* Vol. **37**(4). pp. 1197-1203.

Sunantara, J.D., and J.A. Ramirez. 1997. "Optimal Stochastic Multicrop Seasonal and Intraseasonal Irrigation Control." *Journal of Water Resources Planning and Management.* Vol. **123**(1). pp. 39-48.

Tsuji, G.Y., G. Uehara, and S. Balas (eds.). 1994. *Decision Support System for Agrotechnology Transfer, Version 3*. University of Hawaii, Honolulu.

Tsuji, G.Y., G. Hoogenboom, and P.K. Thornton (eds.). 1998. *Understanding Options for Agricultural Production.* Kluwer Academic Publishers, Dordrecht, Netherlands.

U.S. Department of Agriculture (USDA). 1970. "Irrigation Water Requirements." SCS Engineering Division Technical Release 21 (rev. 2).

Wardlaw, R., and J. Barnes. 1999. "Optimal Allocation of Irrigation Water Supplies in Real Time." *Journal of Irrigation and Drainage Engineering.* Vol. **125**(6). pp. 345-354.

Wilkerson, G.G., J.W. Jones, K.J. Boote, K.T. Ingram, J.W. Mishoe. 1983. "Modeling Soybean Growth for Crop Management." *Transactions of the American Society of Agricultural Engineers*. Vol. **26**(1). pp. 63-73.

Woodruff, C.M., M.R. Peterson, D.H. Schnarre, and C.F. Cromwell. 1972. "Irrigation Scheduling with Planned Soil Moisture Depletion." *ASAE Paper No. 72-722.* American Society of Agricultural Engineers, St. Joseph, Michigan.